



**British  
Geological Survey**

NATURAL ENVIRONMENT RESEARCH COUNCIL

# Additional Soil Gas Monitoring at the Weyburn unit 2003

## Task 2.8 Report for PTRC

Sustainable Energy and Geophysical Surveys Programme

Commissioned Report CR/03/326N





BRITISH GEOLOGICAL SURVEY

COMMISSIONED REPORT CR/03/326N

# Additional Soil Gas Monitoring at the Weyburn unit 2003

## Task 2.8 Report

D. G. Jones, S. Beaubien, M. H. Strutt, J.-C. Baubron, C. Cardellini,  
S Lombardi, F. Quattrochi and L. Penner

*Key words*

Report; key; words.

*Front cover*

Cover picture details, Soil gas  
measurement at suspended Well  
2-25, Weyburn field.

*Bibliographical reference*

D G JONES, S. BEAUBIEN, M H  
STRUTT, J-C BAUBRON, C  
CARDELLINI, S LOMBARDI, F  
QUATTROCHI AND L PENNER.  
2003. Additional Soil Gas  
Monitoring at the Weyburn unit  
2003: Task 2.8 Report. *British  
Geological Survey Commissioned  
Report*, CR/03/326N. 40pp.

## BRITISH GEOLOGICAL SURVEY

The full range of Survey publications is available from the BGS Sales Desks at Nottingham and Edinburgh; see contact details below or shop online at [www.thebgs.co.uk](http://www.thebgs.co.uk)

The London Information Office maintains a reference collection of BGS publications including maps for consultation.

The Survey publishes an annual catalogue of its maps and other publications; this catalogue is available from any of the BGS Sales Desks.

*The British Geological Survey carries out the geological survey of Great Britain and Northern Ireland (the latter as an agency service for the government of Northern Ireland), and of the surrounding continental shelf, as well as its basic research projects. It also undertakes programmes of British technical aid in geology in developing countries as arranged by the Department for International Development and other agencies.*

*The British Geological Survey is a component body of the Natural Environment Research Council.*

### **Keyworth, Nottingham NG12 5GG**

☎ 0115-936 3241 Fax 0115-936 3488  
e-mail: [sales@bgs.ac.uk](mailto:sales@bgs.ac.uk)  
[www.bgs.ac.uk](http://www.bgs.ac.uk)  
Shop online at: [www.thebgs.co.uk](http://www.thebgs.co.uk)

### **Murchison House, West Mains Road, Edinburgh EH9 3LA**

☎ 0131-667 1000 Fax 0131-668 2683  
e-mail: [scotsales@bgs.ac.uk](mailto:scotsales@bgs.ac.uk)

### **London Information Office at the Natural History Museum (Earth Galleries), Exhibition Road, South Kensington, London SW7 2DE**

☎ 020-7589 4090 Fax 020-7584 8270  
☎ 020-7942 5344/45 email: [bgs london@bgs.ac.uk](mailto:bgs london@bgs.ac.uk)

### **Forde House, Park Five Business Centre, Harrier Way, Sowton, Exeter, Devon EX2 7HU**

☎ 01392-445271 Fax 01392-445371

### **Geological Survey of Northern Ireland, 20 College Gardens, Belfast BT9 6BS**

☎ 028-9066 6595 Fax 028-9066 2835

### **Maclea Building, Crowmarsh Gifford, Wallingford, Oxfordshire OX10 8BB**

☎ 01491-838800 Fax 01491-692345

### *Parent Body*

### **Natural Environment Research Council, Polaris House, North Star Avenue, Swindon, Wiltshire SN2 1EU**

☎ 01793-411500 Fax 01793-411501  
[www.nerc.ac.uk](http://www.nerc.ac.uk)

# Foreword

This report describes soil gas monitoring carried out in autumn 2003 in and around the Phase A1 injection area of the Weyburn Oilfield. The work forms Task 2.8 of the Weyburn CO<sub>2</sub> project and entailed additional soil gas studies funded through the Petroleum Technology Research Centre. It extends the main soil gas studies at Weyburn undertaken with European Commission funding under the EU 5<sup>th</sup> Framework Programme. The investigations were carried out by the British Geological Survey (D G Jones, M H Strutt), the University of Rome La Sapienza (S Beaubien, S Lombardi) and Istituto Nazionale di Geofisica e Vulcanologia (C Cardellini, F Quattrochi) from Italy, and the Bureau de Recherches Géologiques et Minières (J-C Baubron) from France with assistance from J D Mollard and Associates (L Penner) from Canada.

# Acknowledgements

The authors would like to thank the many staff of Encana who helped the fieldwork go smoothly, organised land access and surveying and provided field support. In particular we would like to acknowledge the invaluable assistance provided by Ken Ferguson. All the sites were surveyed by Condon Surveying Group, with special thanks to Lowell Peterson

# Contents

|   |           |
|---|-----------|
| <b>Foreword</b> .....                         | <b>i</b>  |
| <b>Acknowledgements</b> .....                 | <b>i</b>  |
| <b>Contents</b> .....                         | <b>i</b>  |
| <b>Summary</b> .....                          | <b>iv</b> |
| <b>1 Introduction</b> .....                   | <b>4</b>  |
| 1.1 Background Site .....                     | 5         |
| 1.2 Decommissioned wells .....                | 6         |
| 1.3 River lineament profiles .....            | 6         |
| 1.4 Salt collapse structure .....             | 6         |
| <b>2 Materials and Methods</b> .....          | <b>7</b>  |
| 2.1 Soil gas method .....                     | 7         |
| 2.2 Gamma spectrometry .....                  | 8         |
| 2.3 Data processing.....                      | 8         |
| <b>3 Results and Discussion</b> .....         | <b>8</b>  |
| 3.1 Data intercomparisons .....               | 9         |
| 3.2 Grid sampling at the background site..... | 9         |

|                         |   |           |
|-------------------------|---|-----------|
| 3.3                     | Grid sampling around the abandoned wells .....    | 11        |
| 3.4                     | Profiles across the river lineaments .....        | 12        |
| 3.5                     | Profiles across the salt collapse structure ..... | 12        |
| <b>References .....</b> |   | <b>13</b> |

## FIGURES

Figure 1. Locations of additional soil gas sites in relation to main grid 18

Figure 2. Normal probability plot showing the method used for defining data set populations for laboratory analysed gases, with CO<sub>2</sub> values obtained over the main grid as an example. Note that the boundaries defined for the main grid have been used for the plotting of all studied sites in order to facilitate comparisons and to put the various values in a more regional context. 19

Figure 3. Box and whisker plot showing the statistical distribution of the laboratory datasets. The plot consists of a central horizontal line defining the median, a coloured box outlining the lower and upper quartiles, two 'whiskers' showing the 'normal' minimum and maximum values, and a series of blue lines defining outlier values. Abbreviations are as follows: grid - main grid over the CO<sub>2</sub> injection area, bg - background site, w - decommissioned wells, hp - horizontal profiles over the river lineament, scs - salt collapse structure. 20

Figure 4. Box and whisker plot showing the statistical distribution of the BGS field data sets. The plot consists of a central horizontal line defining the median, a coloured box outlining the lower and upper quartiles, two 'whiskers' showing the 'normal' minimum and maximum values, and a series of blue lines defining outlier values. 'Notches' on the boxes show significant differences between the medians of groups at the approximately 95% confidence level. Abbreviations are as follows: grid - main grid over the CO<sub>2</sub> injection area, bg - background site, w - decommissioned wells, hp - horizontal profiles over the river lineament, scs - salt collapse structure. 21

Figure 5. Data comparisons for additional soil gas work: a) Laboratory CO<sub>2</sub> (URS) v field CO<sub>2</sub> (BRGM); b) the two field Rn methods; c) Rn v CO<sub>2</sub> 22

Figure 6. Gamma spectrometer traverses (black) and soil gas sample points (purple) for the background area near Minard's Farm 23

Figure 7. Comparison of gamma spectrometer data for the Background Site (Minard's Farm) and Main Grid areas 24

Figure 8. Contour maps of data from the background site, which is located on the western side of Highway 35 approximately 10 km to the north east of the Encana site. Plots show elevation (a), CO<sub>2</sub> (b) and COS (c) distributions using the colour schemes and population divisions defined for the main grid data. Note that CO<sub>2</sub> values do not occur in the "highly anomalous" yellow field, and that all three spot anomalies occur in correspondence with elevation lows. COS values are consistently low compared to the main grid data. (continued on next page). 25

Figure 9. Plots showing: a) Rn, b) Tn and c) field CO<sub>2</sub> for the background site at Minard's Farm. Note that there are broad similarities between the patterns of the gases, but also some differences in detail 27

Figure 10. Contour maps of data from the two studied decommissioned wells. Plots show CO<sub>2</sub> and CH<sub>4</sub> distributions for well 12-18 (a and c) and for well 2-25 (b and d) using the colour schemes and population divisions defined for the main grid data. Note that CO<sub>2</sub> in well 2-25

(b) and CH<sub>4</sub> in well 12-18 (c) exhibit very few background values. (continued on next page).  
28

Figure 11. Contour maps of: a) Rn, b) Tn and c) field CO<sub>2</sub> distributions for abandoned well 12-18. Note the generally low levels of all gases and few features in common between CO<sub>2</sub> and the other gases 30

Figure 12. Contour maps of: a) Rn, b) Tn and c) field CO<sub>2</sub> distributions for abandoned well 2-25. Note that although two of the three points with highest CO<sub>2</sub> also have higher Rn and Tn, there are other relatively high Rn and Tn values associated with lower CO<sub>2</sub> levels 31

Figure 13. Soil gas results from the two horizontal profiles performed across a river lineament (chosen by JD Mollard and Associates) to the north of the main soil gas grid. Note the correspondence between elevation and CO<sub>2</sub> concentrations for both profiles. The lack of correspondence with other gases (except one ethylene peak on profile H), however, implies a shallow biogenic origin for the CO<sub>2</sub> due to the moist, organic rich soil in the valley and in various small depressions. 32

Figure 14. Field soil gas results from the two horizontal profiles performed across a river lineament (chosen by JD Mollard and Associates) to the north of the main soil gas grid. Note the general lack of higher Rn and Tn where CO<sub>2</sub> is higher and the lower O<sub>2</sub> values, implying a biogenic origin for the CO<sub>2</sub> associated with vegetated areas of the valley floor and small depressions 33

Figure 15. Laboratory CO<sub>2</sub> and He (field laboratory) data for Profile G across the river lineament. Only He values clearly above the atmospheric level of 5.24 ppm are shown. Note the coincidence of a He anomaly with the main occurrence of higher CO<sub>2</sub>, but that other He anomalies are associated with very low levels of CO<sub>2</sub> 34

Figure 16. Laboratory soil gas results from the two horizontal profiles performed across the salt collapse structure chosen by JD Mollard and Associates. Note that these data are plotted at the same scale as those in Figure 13 for comparative purposes. In general the lack of variation in the topography of this site is mimicked by the basically flat trends of the soil gas concentrations, particularly CO<sub>2</sub>. Three He anomalies from field laboratory data are shown (red dots) on the E-W He profile. They do not match any features in other gases 35

Figure 17. Field Soil gas results from the two horizontal profiles performed across the salt collapse structure chosen by JD Mollard and Associates. 36

## TABLES

Table 1 Summary of the sites examined during this study. Note that data from the main grid, collected within the principle Weyburn project, are also included for comparative purposes 14

Table 2 Population concentration ranges for the various measured gases, as defined by slope changes observed in normal probability plots of data from the main grid. 15

Table 3 Summary of main statistical parameters for all laboratory analysed gases at all studied sites in 2003, including, for comparative purposes, the main soil-gas grid. Note that hp refers to the horizontal profiles conducted over the river lineament, scs stands for salt collapse structure and w refers to the two decommissioned wells. 16

Table 4 Summary of main statistical parameters for selected field-measured gases and gamma spectrometry results at all studied sites in 2003, including, for comparative purposes, the main soil-gas grid. Note that hp refers to the horizontal profiles conducted over the river lineament, scs stands for salt collapse structure and w refers to the two decommissioned wells. 17

# Summary

The International Energy Agency (IEA) Weyburn project is an international project that is studying the feasibility of long-term geological storage of carbon dioxide (CO<sub>2</sub>), allied to an enhanced oil recovery operation, by Encana, in the Weyburn oilfield, south-eastern Saskatchewan, Canada. CO<sub>2</sub> is being injected into the oil reservoir to improve oil production, whilst at the same time the process should lead to long term geological storage of large volumes of CO<sub>2</sub>. Soil gas studies are being undertaken as part of an EU-funded component of this project, with the primary objective of assessing whether any leakage to surface of injected CO<sub>2</sub> has occurred. This report describes the results of some additional work, funded through the Petroleum Technology Research Centre. The extra work had two main objectives: a) to measure soil gases in a background area, away from the injection zone, with similar ground conditions and b) to investigate possible conduits for leakage of CO<sub>2</sub>.

A background site was chosen about 10km NW of the main soil gas study area, away from the 1A injection panel where the main soil gas studies have been undertaken over the past 3 years. In addition some more detailed measurements were done around two abandoned wells (one completely abandoned, the other suspended), a river lineament and a salt collapse structure. These all might represent possible vertical pathways for gas escape from depth.

In general, the background site showed a similar range of soil gas concentrations to the main study grid, with radon, thoron and some heavier hydrocarbon gases having slightly higher values. This confirms that the levels seen over the CO<sub>2</sub> injection area are normal for such prairie soils and lends further support to the body of evidence indicating a biogenic origin for the CO<sub>2</sub>.

Soil gas concentrations for the two wells were well within the range of data from the main soil gas grid, but the suspended well had, on average, somewhat higher CO<sub>2</sub> values, and the completely abandoned well slightly higher methane and ethane contents than the grid. However, sites around the wells with higher CO<sub>2</sub> or methane/ethane were not associated with higher levels of other gases, such as the highly mobile tracer gas helium, radon or other hydrocarbons. Although small scale leakage cannot be ruled out, there is no strong evidence for it. Further investigation would, however, be warranted to better understand the results.

The river lineament shows some weak CO<sub>2</sub> anomalies but their position, and the general lack of accompanying higher levels of other gases, support a biogenic origin, rather than being indicative of deep gas escape. There are some He anomalies on one profile across the lineament and more detailed work (closer spaced sampling) could be undertaken in future.

The salt collapse structure has generally low concentrations of soil gases and no significant levels, except for some anomalous He results on one profile that merit further investigation.

Overall, there is no evidence so far for escape of injected CO<sub>2</sub> from depth. Further monitoring of soil gases is necessary to verify that this is the case in future and more detailed work is required to better understand the causes of variation in soil gas contents, and investigate further, possible conduits for gas escape.

## 1 Introduction

The International Energy Agency (IEA) Weyburn project is an international project that is studying the feasibility of long-term geological storage of carbon dioxide (CO<sub>2</sub>), allied to an enhanced oil recovery (EOR) operation, by Encana, in the Weyburn oilfield, south-eastern Saskatchewan, Canada. As part of an EU component of the project, the British Geological Survey (BGS), the University of Rome La Sapienza (URS) and Instituto Nazionale di Geofisica

e Vulcanologia (INGV) from Italy, and the Bureau de Recherches Géologiques et Minières (BRGM) from France have carried out annual soil gas surveys, and longer term monitoring, over part of the Phase A1 CO<sub>2</sub> flood area. The objectives of this work are to:

- Establish baseline soil gas values using grid sampling and profiles over anomalies
- Evaluate natural variations in soil gas including seasonal effects
- Compare baseline data with future datasets
- Identify sites of higher gas flux that may be indicative of deep gas escape
- Enable long term monitoring to evaluate possible escape of injected CO<sub>2</sub>
- Address possible public concerns over geological storage of CO<sub>2</sub>

Soil gas surveying, as the name implies, is the collection of gas samples from the unsaturated (or vadose zone) of the soil profile in order to measure the concentration or flux of various gas species. The primary use of this data is to understand geochemical reactions and gas flow pathways in geological sequences. The method has numerous advantages, such as ease of sampling, cost effectiveness and the potential for an unlimited number and density of sampling points, and it is often used alongside more traditional geochemical, geophysical and geological methods in site studies. The method was considered particularly applicable for the present study as it has often been used for the exploration of new oil and gas deposits (e.g. Phip and Crisp, 1982; Jones and Drozd, 1983; Klusman, 1993).

In terms of its application to the present study, this method has been used to address two principal questions that have arisen during work on the main soil gas grid above the Phase A1 CO<sub>2</sub> injection area (hereafter referred to as the ‘main grid’) over the last three years. The first involves the need to better understand the background soil gas concentrations in the agricultural fields of this part of southern Saskatchewan, without the added complication of 50 years of oil-field infrastructure and the ongoing CO<sub>2</sub> flood. A further aim is to assess whether soil gas values for the injection area are in the same range as those from similar areas away from the main Weyburn field (accepting that it is difficult, in this area, to get away completely from oil wells). The second question regards specific man-made or natural vertical structures which may act as conduits for upwardly migrating gases, such as the injected CO<sub>2</sub>. As the main grid has a sample spacing of 200 m it is possible that soil gas anomalies related to small scale features might be missed, and thus a number of sites were selected on the basis of geological and infrastructure considerations for more detailed sampling.

A total of 4 types of sites were chosen, including a background site, decommissioned wells, river lineaments and a salt collapse structure (Figure 1). In addition to these locations, some data from the main grid (collected during the 3-year Weyburn project) is presented for comparative purposes. A brief description of each site, why it was chosen and a summary of the work done there is given below and in Table 1.

## 1.1 BACKGROUND SITE

As described above, data from a site similar to the Encana phase A1 injection area, yet largely undisturbed by oil exploration and extraction, was needed in order to better interpret the results from the main grid. As much of the data collected thus far appears to indicate that the soil gas concentrations observed over the last three years can be attributed to shallow biological and microbiological respiration pathways, an undisturbed site was needed which had similar soil and crop types, soil moisture contents and topography. The chosen site is located north of Minard’s Farm, along Highway 35 (Sections 17 and 20, Township 7, Range 14), approximately 10 km to the north west of the main grid (Figure 1) Although similar in many ways it should be pointed that the main grid has much more surface water and swampy depressions than the background site; these marshy areas are typically associated with higher CO<sub>2</sub> levels. Due to logistical

considerations it was not possible to duplicate the main grid over the background site, but approximately 10% of the grid's samples were collected in an area of about 2.5% of the grid.

## **1.2 DECOMMISSIONED WELLS**

One concern with regards to the possible leakage of the injected CO<sub>2</sub> to surface is that the over 600 oil wells drilled over the last 50 years may provide a vertical migration pathway should borehole / casing seals be chemically or mechanically compromised. Two very different, inactive well sites were chosen (Figure 1), in collaboration with Encana personnel, in order to see if any evidence could be found for gases leaking to the shallow environment from the oil reservoir at depth. The first site, Well 12-18, is completely abandoned; the hole has been cemented shut, the related infrastructure removed and top soil imported to return the site to its original agricultural use. This site, in a grassy field that has been used for pasture for at least the last three years, is located almost in the centre of the main soil gas grid. In contrast, Well 2-25 suffered a casing failure and its operations have been suspended prior to full abandonment. All infrastructure is still in place at this site, including the pump jack (see cover photo), and the gravel access-road / pad is surrounded by a wheat field. Trees bound the southern side of the sampling area, while a small weed-filled depression marks the eastern edge. A total of 16 samples were collected from both sites on a regular 100 m by 100 m grid.

## **1.3 RIVER LINEAMENT PROFILES**

Detailed air-photo and satellite image interpretation of the Weyburn field by J.D. Mollard and Associates (Regina, Saskatchewan) has outlined a number of lineaments in the area. They are defined by elongated surface water bodies, straight river sections, tonal contrasts and other linear features. While some of these features could be related to shallow processes, such as glacial scouring, lateral lithological variations or even human intervention, it is possible that some may be surface expressions of deep faults. There is a close correspondence between the location and orientation of the lineaments and faulting in the Midale Beds (Task 2.6 report). As a result, these structures could provide a conduit for the migration of gases to the surface, including the injected CO<sub>2</sub>. A straight, SW-NE trending section of the seasonal Roughbark Creek was selected for study, and two detailed horizontal soil gas profiles (named G and H) were performed across the water body to monitor for anomalous gas concentrations associated with the lineament (Figure 1). Sample spacing was chosen to maximize detail near the creek while still providing data from 'background' areas further away, thus it varied from 10 m near the creek to 50 m at the ends of the profiles away from the lineament. The profiles predominantly crossed grassy pasture, but some small weed-filled depressions, and brush, bulrushes and other marsh vegetation occurred in the valley (about 3m deep) near to standing water.

## **1.4 SALT COLLAPSE STRUCTURE**

Other possible conduits for upwardly migrating gases are deep geological features that can be seen in some of the many seismic surveys that have been performed over the Encana oil field. One such feature, highlighted by J.D. Mollard and Associates, is a salt collapse structure within the Prairie Evaporite. This collapse structure can clearly be observed on seismic sections as a series of vertical offsets that extend slightly, at least at the resolution of the survey, into the overlying unit. The deep structure is related spatially to lineament zones identified from satellite data (Task 2.6 report). Two horizontal profiles were performed above this structure, with each profile consisting of 10 samples spaced 25 m apart; the profiles crossed each other in the middle forming a NS-EW trending plus sign. The two perpendicular profiles were performed just south of the Encana operations plant in a very flat, homogenous wheat field (see Figure 1 for location).

## 2 Materials and Methods

### 2.1 SOIL GAS METHOD

The probe used to collect soil gas samples consisted of a modified ¼ inch, thick-walled, stainless-steel tube onto which two steel cylinders were welded to act as pounding surfaces when installing and removing the probe with a co-axial hammer. The bottom end of the probe was fitted with a sacrificial tip to prevent blockage of the tube during insertion into the ground. The top end was left open so that a septum holder or silicone tubing could be attached for collecting gas samples.

The sampling procedure (see Lombardi et al., 1996 and Ciotoli et al., 1999) involved hammering the probe to a depth that is not influenced by the input of atmospheric gases via diffusion or barometric pumping (Hinkle, 1994); at Weyburn this was determined to be between 60 and 90 cm below ground surface on the basis of vertical profiling. A small bellows pump was then attached to the upper end and evacuated, and then the probe was gently tapped upwards in order to release the sacrificial tip. Once the bottom of the probe was free of the tip and within a gas permeable horizon the bellows pump would fill with air, indicating that it was possible to sample. The bellows were then pumped twice to clean the probe of any atmospheric air, a septum holder was attached to the open end of the tube, the needle of a 60ml plastic syringe was inserted through the septum and a 60ml gas sample was drawn up and injected into a previously evacuated stainless steel container. These containers were then transported back to the laboratory and analysed for hydrocarbon species (C1-C3 alkanes and C<sub>2</sub>H<sub>4</sub>), sulphur species (COS and SO<sub>2</sub>) and permanent gases (N<sub>2</sub>, O<sub>2</sub> and CO<sub>2</sub>) using two Fisons 8000-series bench gas chromatographs, as well as He using a Varian helium leak detector. After the septum holder was removed gas was pumped via a bellows pump into a Pylon AB5 radon monitor, for the analysis of radon and thoron, and then the probe was attached to a Geotechnical Instruments Analox Infrared gas analyser for the measurement of CO<sub>2</sub> and O<sub>2</sub> (plus barometric pressure) directly in the field.

Gases were also pumped from the probe at a flow rate of 0.2 l.min<sup>-1</sup>. They were analysed for CO<sub>2</sub> directly on line, and for Rn and He from a 1 L Teflon bag inflated on site. The second field analysis of CO<sub>2</sub> was made using an infra-red spectrometer (LFG20, UK-ADC) with a sensitivity of 2 %. He was measured in a field laboratory by specific mass spectrometry (100HDS, F-Alcatel) with a sensitivity of +/- 0.01 ppm. The He data were normalised to atmospheric air concentration (5.24 ppm) at local pressure between each sample. Results were verified using gas standards before and after the field campaign. Rn was also measured in the field laboratory (without Tn) using 125 ml ZnS scintillating bottles and a Calen counting chain (F-Algade) with a 10 minute accumulation time after 3 hours delay for equilibrium of Rn daughters and decay of thoron products. With such conditions, Rn accuracy of sampling and measurement is usually better than 10%.

Measurement of CO<sub>2</sub> flux was made by the accumulation chamber method using an IRGA LI-COR 800 instrument equipped with an optical bench (LI-COR 800-905) set to work in the range 0-5000 ppm.

Due to the high density of buried infrastructure all sampling points were chosen in consultation with Encana personnel and the agreed points were geophysically surveyed for buried structures and located with GPS (to an accuracy of a few cm) by Condon Surveying.

## 2.2 GAMMA SPECTROMETRY

Gamma spectrometry was carried out at the Minard's background site and part of the main grid area. For the purposes of the present work, this was primarily done to establish that the soils at the two locations were similar. This technique measures U and Th series radionuclides (as well as K and total gamma) and hence there is a link to radon and thoron measurements. There can be a coincidence between anomalies of these gases and gamma anomalies, for example where structures, such as faults, are associated with gas escape. It has also been shown that gas leakage, can cause alteration of surface soils, changing levels of K, U and Th (e.g. Klusman, 1993; Tedesco, 1995; Schumacher and Le Schack, 2002). The instrument used (an Exploranium GR320 with 76 x 76 mm NaI(Tl) detector) can be operated in static mode, or continuous measurements taken while the operator walks slowly across the ground. Positioning in continuous mode was obtained using a handheld GPS receiver (with an accuracy of a few m). In this mode there is the potential to detect features missed by point gas sampling. Both styles of operation were used on the main grid, but only continuous traverses at the background site. Lack of access to the other sites, when this instrument was being deployed, prevented further work being carried out.

## 2.3 DATA PROCESSING

All the soil gas data was first examined statistically using the software packages Statistica (Statsoft), Microsoft Excel and S-Plus both via the creation of tables as well as statistical plots. This approach allowed a rigorous comparison between the various data sets in order to define trends or anomalous distributions. This was mainly accomplished through the use of normal-probability plots (NPP) and box-whisker plots (BWP). An NPP, created by plotting observed residuals versus observed concentration values, is used to evaluate whether and to what extent the distribution of a variable follows a normal distribution. If the data is normally distributed then all values should fall onto a straight line, however if the data is not normal then flexure points between linear segments can be used to define sub-populations which may be the result of different origins, controlling mechanisms or transport pathways (Sinclair, 1991). The NPPs were mainly used to interpret the large data set from the main grid, and then the resulting population boundaries were used to subdivide (and plot) the other data sets. This approach allows for a more objective, easier comparison between both detailed and regional sites. An example of the NPP procedure followed to define the various populations is given in Figure 2 for the main grid's CO<sub>2</sub> values, while Table 2 outlines the concentration ranges and colour fields defined for each population for each gas. In contrast to the NPPs, BWPs are very useful for the visual comparison of entire data sets. These plots (e.g. Figures 3 and 4), which compare the statistical distribution of a single gas from different sites, consist of a central line marking the median concentration, box extremes marking the upper and lower quartiles, 'whisker' extremes marking the 'normal' maximum and minimum values, and individual symbols showing outlier values that lie outside the whiskers. In addition to the statistical processing of the data, all results were plotted using the software packages Surfer and ArcView, for the gridded data, and Grapher, S-Plus or Excel for the horizontal profile results.

## 3 Results and Discussion

As outlined in the introduction, the sites examined in this work were chosen in an effort to maximize the information coming from the larger soil gas research being conducted on the Weyburn CO<sub>2</sub> injection site. In particular this work addresses some of the questions that have arisen regarding natural soil gas distribution for the area as well as to target specific sites which may represent possible natural or man-made migration pathways. In order to put these site-

specific data sets in context, however, it is necessary to make reference to the much larger data set collected from the soil gas grid above the CO<sub>2</sub> injection area (i.e. the “main grid”) during the same period. One obvious approach for this comparison is through the use of statistics, although it must be stated clearly that a fundamental weakness in this approach for the present data is the fact that each ‘mini-site’ has much fewer sample points (5 to 10 %) collected over much smaller areas than the main grid, and thus there is the potential for data bias. That said this comparison, in general, shows excellent correspondence between the various studied sites and thus provides a good starting point for the discussion.

The statistical distribution of the collected data are presented in tabular form for all laboratory-analysed gases in Table 3 as well as in graphical form for some selected species in Figure 3. Some of the field measurements are summarised in Table 4. The “box and whisker” plots given in Figures 3 and 4 are a convenient way to quickly assess statistical variations between populations. This graph will be referenced extensively in the discussion below on the specific sites, although one must always consider the number of samples collected from each site, as listed in Tables 3 and 4.

### **3.1 DATA INTERCOMPARISONS**

The two field CO<sub>2</sub> measurements are generally in good agreement with the more precise laboratory results (e.g. Figure 5). They provide a useful confirmation of the integrity of the stainless steel sample containers; significant discrepancies indicating potentially leaky canisters from which data should be treated with caution. The correlation also demonstrates that it would be appropriate to use the field measurements systematically to select areas for more detailed study during a field campaign.

The two sets of Rn measurements do not correlate as well as the CO<sub>2</sub> data (Figure 5. ). The Pylon measurements provide data for Tn as well as Rn and involve shorter counting times. They are likely to have lower precision than the longer counts for Rn alone, but are suitable as a rapid method providing almost instant results. The relationship between the two Rn datasets is being investigated further as part of the main EC-funded soil gas work.

The plot of Rn concentration relative to CO<sub>2</sub> (Figure 5) shows a generally poor correlation between the two gases. The obvious large scatter is consistent with a mainly diffusion-driven gas flow at most of the sites analysed, a more direct relationship between CO<sub>2</sub> and Rn would indicate advective processes, with CO<sub>2</sub> acting as a carrier for Rn.

### **3.2 GRID SAMPLING AT THE BACKGROUND SITE.**

Gamma spectrometer traverses were carried out at the site to compare soil composition to the main grid and to investigate whether there were any anomalies that might be related to radon and thoron features. This work was undertaken before the soil gas sampling points had been surveyed in, but managed to cover almost two thirds of the soil gas area (Figure 6). There was not time to acquire complete coverage.

The gamma data show a range of values within that from the main grid area (Figure 7). There are however slight but significant differences revealed by the statistics (Table 4), which show higher mean (and median) K, U and Th and Total Count for the background area. The two sets of values do show a strong overlap and, bearing in mind that the data from the main grid only cover a fraction of the total area, they are sufficiently similar to suggest that the background site is a reasonable choice, with similar characteristics to the main grid.

Elevation data for the background site is presented in Figure 8a whereas the laboratory soil gas values for this site are contoured in Figures 8b through 8g.

The distribution of CO<sub>2</sub> in Figure 8b shows a “spotty” distribution of its anomalies, with high values being located to the SE, near the dugout, and in the NW and NE corners. These sites reach maximum values of between 0.9 and 1.3 % and clearly correspond with the lowest points on the survey grid (Fig.8a), implying biological activity in the moister, more organic-rich depressions (Boone et al., 1998; Bouma and Bryla, 2000; Risk et al., 2002). When these background data are compared to those from the main grid (Fig. 3a) one can see that the statistical distributions are very similar, with the main difference being the larger number of outliers (i.e. a more skewed distribution) occurring in the latter, up to a maximum value of 2.2%. Although this slight difference could be interpreted as being due to a separate source at the main grid, such as deep CO<sub>2</sub> coming from the injection process, a more likely explanation is that the much larger main grid covers a greater range of soil types, crop types and topography (Table 1) and therefore has the potential to sample a wider range of shallow CO<sub>2</sub>-producing environments. This interpretation is supported by other evidence collected within the framework of the larger soil gas project, including location of CO<sub>2</sub> anomalies over the large grid, vertical profiles results, O<sub>2</sub>-N<sub>2</sub> distributions and isotopic data. The data for the background site also show only atmospheric levels, with no indication of any addition from a deeper source. The greater number of outliers in the grid data is also consistent with the much larger number of measurements.

Rn and Tn levels are slightly higher for the background site compared to the grid (Figure 4, Table 4) as is the case for U and Th series radionuclides measured by gamma spectrometry. This suggests slight differences in soil composition between the two areas, given the dry conditions during measurement at both sites and the generally similar soil types, implying comparable permeabilities. Slightly higher Rn values are associated with the areas of higher CO<sub>2</sub>, but equally, similar levels are seen where CO<sub>2</sub> concentrations are relatively low (Figure 9). The relationship between Tn and CO<sub>2</sub> is similarly not clear cut.

The concentrations of carbonyl sulphide (Figure 8c) are very low, with only one sample lying within the “anomalous” range defined on the basis of the main grid data. Examination of box and whisker plot in Figure 3f, indicates that there is no statistical difference between these two data sets.

Perhaps more interesting is the distribution of the various hydrocarbon gases analysed, with methane exhibiting a unique distribution of generally low concentrations (Figure 8d), whereas ethylene, ethane and propane (Figure 8e-g) all show a similar distribution and the occurrence of some relatively elevated values. Although all hydrocarbon gases from the background site show a similar statistical distribution compared to the main grid (Fig. 3 b-e) both ethylene and propane from the former site show outlier values that are much higher than those from the latter, as shown by the classed post symbols in the contour plots. This result supports the interpretation that there are few natural leakage pathways above the CO<sub>2</sub> injection site, as one would expect these heavier hydrocarbons to occur at higher concentrations above a 50 year old oil field (having over 600 boreholes penetrating the reservoir) than above an essentially non-producing area. A contrary hypothesis, however, may be that depressurising of the Weyburn field during its long history has actually resulted in lower soil gas concentrations over time, and that the elevated values observed at the background site may be due to migration from an uneconomic or undiscovered reservoir at that location. More research would be required to understand if these gases are due to a shallow or deep source at this location, but such an effect has been observed, particularly for light hydrocarbons (defined as mainly C<sub>1</sub>-C<sub>5</sub> compounds), above other oilfields (e.g. Schumacher and Abrams, 1996; Schumacher and Hitzman, 2001; Schumacher and LeSchack, 2002).

### 3.3 GRID SAMPLING AROUND THE ABANDONED WELLS

Contoured data for all the gases analysed from both studied well sites, that is the fully abandoned 12-18 and the suspended 2-25, are presented in the various plots of Figures 10-12. The distributions of CO<sub>2</sub> and CH<sub>4</sub> in Figures 10 a-d show the exact opposite trend, with the former being elevated around the suspended well whereas the latter is more concentrated above the abandoned well. In fact in both Figures 10b and c there is very little area covered by the “background” population (i.e. white), indicating that these values are elevated with respect to the general distribution observed above the CO<sub>2</sub> injection grid. This is also shown by examination of the statistical distribution of these gases in Figures 3a and b, where CO<sub>2</sub> plots higher for well 2-25 and CH<sub>4</sub> plots higher for well 12-18 when compared to the average distributions found at the other sites. Rn levels, like CO<sub>2</sub> are slightly higher than those for the grid at Well 2-25 (Figure 4), but marginally lower at 12-18, whilst Tn values are not significantly different for either well. There are, however, no corresponding higher Rn or Tn levels to match the higher CO<sub>2</sub> points for Well 2-25 (Figure 12).

In sharp contrast to the results observed over the background site, there is no correlation amongst the heavier hydrocarbon gases, with ethylene showing extremely low background concentrations as compared to the weakly to strongly anomalous values of ethane. In addition, whereas methane showed no correspondence with the other hydrocarbons at the background site there is a clear relationship between methane and ethane above both well sites, as can also be seen in the elevated distributions of both gases at well 12-18 in Figure 10b and d.

In general it should be noted that none of the four gases exhibit elevated outlier concentrations outside the range of values observed above the main grid, however what is observed is that the *populations* as a whole for CO<sub>2</sub> at the suspended well, and CH<sub>4</sub> and C<sub>2</sub>H<sub>6</sub> at the abandoned well are elevated with respect to that observed for the other sites. As stated previously care must be taken in interpreting this type of data due to the biases which may result from the small area and small number of samples collected. For the suspended well 2-25, no previous soil gas surveys have been conducted in this area, and thus it is not possible to compare these detailed site results with those from the surrounding area. As such the elevated CO<sub>2</sub> population (as opposed to the relatively moderate concentrations) observed above this site are difficult to put into context. That said the lack of corresponding anomalies in the other measured gases, in particular the highly mobile CH<sub>4</sub>, implies that these values are not due to direct leakage from depth along the failed casing. The values for this well site were also all at background atmospheric levels. Some higher Rn values are associated with higher CO<sub>2</sub> levels, but similar Rn concentrations also occur with much lower CO<sub>2</sub> (Figure 12).

Whereas well 2-25 is located to the north of the main grid, well 12-18 is within this grid and thus there exists three years of data for the area surrounding this lease. This area has consistently yielded very low CO<sub>2</sub> values, in agreement with the background to weakly anomalous values observed above the former well head (Fig. 10a). Ethylene, as well, shows very low values in both the detailed and more regional grids. However, the values of methane and especially ethane from the detailed grid are anomalously high for the area. This can be illustrated by examining the four main-grid points that surround the detailed grid, located each about 150m from the original well-head location. Methane values are slightly higher for the detailed grid (1 to 3.39 ppm) compared to the four surrounding points (1.4 to 2.1 ppm), whereas ethane values are significantly higher (0.02 to 0.08 ppm as compared to 0.01 to 0.02 ppm, respectively). Again it must be stressed that none of the values observed for the hydrocarbon gases above abandoned well 12-18 are outside the range of values observed for the grid as a whole, only that methane and ethane are elevated with respect to the surrounding area. Present data does not allow for a clear definition as to the cause of this difference, however possibilities include remnant

hydrocarbon pollution or the site's proximity to an ephemeral stream. Although small scale leakage from the underlying reservoir cannot be totally discounted, the anomalies are small and are more likely due to near surface features, an interpretation supported by the lack of a clear helium anomaly in the area (not shown) – only one point gave a slightly anomalous He result (5.29 ppm) and this did not correspond to one of the highest methane values. There are also no matching Rn or Th features (Figure 11).

### 3.4 PROFILES ACROSS THE RIVER LINEAMENTS

Data for the two horizontal profiles (G and H) across the SW-NE river lineament, located just to the north of the main grid, are presented in Figure 13 along with elevation values collected during the surveying of the sampling points. For both profiles there is a clear correlation between topography and CO<sub>2</sub> concentration, with the main river valley (as well as small depressions) having elevated CO<sub>2</sub> values. In contrast there appears to be a weak depression of the CH<sub>4</sub> signal where there are peaks of CO<sub>2</sub>, particularly along profile G. Rn is also lower where CO<sub>2</sub> is higher, whilst Tn is more variable, low for the highest CO<sub>2</sub> on each profile, but relatively high over a weaker CO<sub>2</sub> peak (Figure 14). In general the distribution of the three hydrocarbon species are highly irregular, although there is a weak correlation between CH<sub>4</sub> and C<sub>2</sub>H<sub>6</sub> for profile G which is not duplicated in profile H. Instead in profile H there is a clear correspondence between CO<sub>2</sub> and C<sub>2</sub>H<sub>4</sub> anomalies located just 2 m beside the river, along with a minimum CH<sub>4</sub> value of 0.037. He, measured in the laboratory, shows no clear trend along profile G, with values oscillating near atmospheric values within the range of instrument error (there is no laboratory He data for profile H due to instrument failure). However, He measured in the field laboratory does show some anomalous values for Profile G (Figure 15). One of these coincides with the highest CO<sub>2</sub> values, but the others, all at the south east end of the profile, are associated with very low CO<sub>2</sub> levels. There were no anomalous He values at all on Profile H.

As outlined in the introduction, these two profiles were conducted in order to see if the river lineament is a surface expression of a structural discontinuity which could act as a conduit for upwardly migrating gases, in particular for the injected CO<sub>2</sub>. If such were the case one would expect to see a pronounced peak of CO<sub>2</sub> in correspondence with the river valley on both profiles, similar to that observed. However, since there are no convincing anomalous values for most of the other gases in correspondence with the lineament (apart from the field laboratory He on Profile G and one C<sub>2</sub>H<sub>4</sub> peak on profile H) evidence for such a conduit is very weak. In particular the lack of a clear-cut relationship between CO<sub>2</sub> and the tracer gas helium, which is associated with the oil reservoir, or CH<sub>4</sub>, both of which are less reactive and far more mobile than CO<sub>2</sub>, indicates that the observed CO<sub>2</sub> peaks are most likely due to near surface biological reactions (Bouma and Bryla, 2000). However, the coincidence of the main CO<sub>2</sub> feature on profile G with an anomalous field laboratory He value does warrant further, more detailed, examination.

### 3.5 PROFILES ACROSS THE SALT COLLAPSE STRUCTURE

The data for the two intersecting (one E-W the other N-S) horizontal profiles conducted above the salt collapse structure, to the east of the main grid, are presented in Figure 16, using the same scales as those used in Figure 13 for the river lineament profiles, and Figure 17. It is very clear that this location, which is an extremely homogenous, flat wheat field with no surface water, shows much less concentration variations when compared to the river lineament data. With no depressions to accumulate water and organic matter, the CO<sub>2</sub> concentrations are monotonously

flat, lending credence to the belief that the CO<sub>2</sub> peaks on the river lineament profiles are due to shallow biological processes. With regard to the other gases, the only recognizable feature is a CH<sub>4</sub>, C<sub>2</sub>H<sub>6</sub>, He and Rn minimum which corresponds to a C<sub>2</sub>H<sub>4</sub> maximum along the N-S profile. There are three small He anomalies in the field laboratory data on the E-W profile but these are not coincident with features in other gases. As to possible leakage along the salt collapse discontinuities, there is no evidence for escape of injected CO<sub>2</sub> or reservoir hydrocarbons along this structure. Levels of gases are typically comparable or lower than those for the main grid.

## References

- BOONE R.D., NADELHOFFER K.J., CANARY J.D. and KAYE J.P. (1998) Roots exert a strong influence on the temperature sensitivity of soil respiration. *Nature*, Vol. 396, 570-572.
- BOUMA T.J. and BRYLA D.R. (2000) On the assessment of root respiration for soils of different textures: interactions with soil moisture contents and soil CO<sub>2</sub> concentrations. *Plant and Soil*. Vol. 227, 215-221.
- CIOTOLI G., ETIOPE G., GUERRA M., LOMBARDI S. (1999) - The detection of concealed faults in the Ofanto Basin using the correlation between soil-gas fracture surveys. *Tectonophysics*, Vol. 301 (3-4), 321-332.
- HINKLE, M. (1994). Environmental conditions affecting concentrations of He, CO<sub>2</sub>, O<sub>2</sub> and N<sub>2</sub> in soil gases, *Applied Geochemistry* Vol. 9, 53-63.
- JONES V.T., DROZD R.J. (1983) - Prediction of oil or gas potential by near-surface geochemistry. *American Association of Petroleum Geologists Bulletin*., Vol. 67, 932-952.
- KLUSMAN R.W. (1993) - Soil gas and related methods for natural resource exploration. J. Wiley & Sons.
- LOMBARDI S., BENEVEGÙ F., BRONDI A., POLIZZANO C. (1993) - Field investigation with regard to the impermeability of clay formations: Helium-4 soil gas surveys in sedimentary basins as a tentative study of secondary permeability in clayey sequences - *Commission of the European Communities, Nuclear Science and Technology. Report EUR 14585 EN*.
- LOMBARDI S., ETIOPE G., GUERRA M., CIOTOLI G., GRAINGER P., DUDDRIDGE G.A., GERA F., CHIANTORE V., PENSIERI R., GRINDROD P., IMPEY M. (1996) :The refinement of soil gas analysis as a geological investigative technique. *Commission of the European Communities, Nuclear Science and Technology. Final report. EUR 16929 EN*
- PHILP R.P. and CRISP P.T. (1982) - Surface geochemical methods used for oil and gas prospecting - A review. *Journal of Geochemical Exploration*, Vol. 17, 1-34.
- RISK D., KELLMAN L., and BELTRAMI H. (2002) Soil CO<sub>2</sub> production and surface flux at four climate observatories in eastern Canada. *Global Biogeochemical Cycles*, Vol. 16(4) 69-80.
- SINCLAIR A.J. (1991). A fundamental approach to threshold estimation in exploration geochemistry: probability plots revisited. *Journal of Geochemical Exploration*, Vol. 41, 1-22.
- SCHUMACHER, D and ABRAMS, M. A., eds. (1996). Hydrocarbon Migration and Its near-Surface Expression : *American Association of Petroleum Geologists Memoir 66*
- SCHUMACHER, D and HITZMAN, D. C. (2001). Geochemical exploration in mature basins: new applications for field development and production. Rock the foundation convention, June 18-22, 2001, Calgary. Canadian Society of Petroleum Geologists, Extended abstract No. 011, 1-8.
- SCHUMACHER, D. and L A. LESCHACK (eds.) (2002). Surface Exploration Case Histories: Applications of Geochemical, Magnetic, and Remote Sensing AAPG Studies in Geology No. 48, SEG Geophysical References Series No. 11
- TEDESCO, S. A. 1995. Surface geochemistry in petroleum exploration. Chapman and Hall, New York

**Table 1 Summary of the sites examined during this study. Note that data from the main grid, collected within the principle Weyburn project, are also included for comparative purposes**

|                                | Number of samples | Sample spacing (m) | Sample area (km <sup>2</sup> ) | Sample density (s/km <sup>2</sup> ) | Dominant vegetation                       | Topography   |
|--------------------------------|-------------------|--------------------|--------------------------------|-------------------------------------|---|--|
| Main grid                      | 360               | 200                | 14.4                           | 25                                  | wheat, weeds, tilled soil, flax, pasture, | much surface water, depressions, undulating ground |
| Background                     | 37                | 100                | 0.35                           | 100                                 | wheat, weeds, tilled soil                 | undulating ground                                  |
| Well 12-18 (no infrastructure) | 16                | 25                 | 0.01                           | 1600                                | pasture                                   | flat   |
| Well 2-25 (infrastructure)     | 16                | 25                 | 0.01                           | 1600                                | wheat, weeds, trees                       | flat with weedy depression                         |
| River lineament profile G      | 36                | 10-50              | -                              | -                                   | pasture, weeds, bulrushes                 | undulating plus river valley                       |
| River lineament profile H      | 29                | 10-50              | -                              | -                                   | pasture, weeds, bulrushes                 | undulating plus river valley                       |
| Salt collapse structure        | 20                | 25                 | -                              | -                                   | wheat                                     | very flat  |

*Table 2 Population concentration ranges for the various measured gases, as defined by slope changes observed in normal probability plots of data from the main grid.*

|                                     | Background<br>(white) | Weak anomaly<br>(pink) | Anomaly<br>(blue) | Strong anomaly<br>(yellow) |
|-------------------------------------|-----------------------|------------------------|-------------------|----------------------------|
| CO <sub>2</sub> (%)                 | 0-0.24                | 0.24-0.51              | 0.51-1.78         | 1.78-2.2                   |
| CH <sub>4</sub> (ppm)               | 0-1.21                | 1.21-1.87              | 1.87-2.9          | 2.9-6.87                   |
| C <sub>2</sub> H <sub>4</sub> (ppm) | 0-0.008               | 0.008-0.026            | 0.026-0.064       | 0.064-0.137                |
| C <sub>2</sub> H <sub>6</sub> (ppm) | 0-0.01                | 0.01-0.031             | 0.031-0.044       | 0.044-0.149                |
| C <sub>3</sub> H <sub>8</sub> (ppm) | 0-0.056               | 0.056-0.126            | 0.126-0.46        | 0.46-0.664                 |
| COS (ppm)                           | 0-0.44                | 0.44-0.66              | 0.66-0.87         | 0.87-1.70                  |

**Table 3 Summary of main statistical parameters for all laboratory analysed gases at all studied sites in 2003, including, for comparative purposes, the main soil-gas grid. Note that hp refers to the horizontal profiles conducted over the river lineament, scs stands for salt collapse structure and w refers to the two decommissioned wells.**

|  | Site       | Valid Number | Mean  | Median | Min.  | Max.  | Lower Quartile | Upper Quartile | Std.Dev. | Percent Std.Dev. |
|--|------------|--------------|-------|--------|-------|-------|----------------|----------------|----------|------------------|
| <b>CH<sub>4</sub></b><br>ppm             | main grid  | 358          | 1.22  | 1.10   | 0.24  | 6.87  | 0.84           | 1.49           | 0.65     | 53.2             |
|  | background | 37           | 1.32  | 1.17   | 0.43  | 2.99  | 0.82           | 1.67           | 0.64     | 48.2             |
|  | hp-g       | 36           | 1.72  | 1.57   | 0.63  | 3.25  | 1.21           | 2.21           | 0.63     | 36.9             |
|  | hp-h       | 29           | 1.13  | 1.08   | 0.04  | 3.75  | 0.82           | 1.25           | 0.65     | 57.7             |
|  | scs        | 20           | 1.10  | 1.09   | 0.00  | 2.23  | 1.01           | 1.19           | 0.39     | 35.5             |
|  | w12-18     | 17           | 1.90  | 1.82   | 1.00  | 3.39  | 1.57           | 2.17           | 0.57     | 30.1             |
|  | w2-25      | 16           | 1.20  | 1.22   | 0.50  | 2.57  | 0.84           | 1.35           | 0.47     | 39.3             |
|  |            |              |       |        |       |       |                |                |          |                  |
| <b>C<sub>2</sub>H<sub>4</sub></b><br>ppm | main grid  | 358          | 0.012 | 0.008  | 0.000 | 0.137 | 0.005          | 0.014          | 0.015    | 123.5            |
|  | background | 37           | 0.027 | 0.006  | 0.000 | 0.354 | 0.004          | 0.010          | 0.077    | 287.4            |
|  | hp-g       | 36           | 0.012 | 0.008  | 0.000 | 0.032 | 0.006          | 0.016          | 0.008    | 70.2             |
|  | hp-h       | 29           | 0.011 | 0.008  | 0.002 | 0.059 | 0.005          | 0.012          | 0.012    | 110.9            |
|  | scs        | 20           | 0.009 | 0.007  | 0.003 | 0.028 | 0.005          | 0.011          | 0.006    | 69.0             |
|  | w12-18     | 17           | 0.009 | 0.006  | 0.000 | 0.020 | 0.005          | 0.012          | 0.006    | 65.0             |
|  | w2-25      | 16           | 0.010 | 0.010  | 0.003 | 0.019 | 0.006          | 0.015          | 0.006    | 53.3             |
|  |            |              |       |        |       |       |                |                |          |                  |
| <b>C<sub>2</sub>H<sub>6</sub></b><br>ppm | main grid  | 358          | 0.022 | 0.019  | 0.000 | 0.149 | 0.011          | 0.028          | 0.015    | 71.1             |
|  | background | 37           | 0.020 | 0.015  | 0.000 | 0.112 | 0.010          | 0.023          | 0.019    | 96.2             |
|  | hp-g       | 36           | 0.032 | 0.031  | 0.014 | 0.069 | 0.023          | 0.039          | 0.011    | 35.7             |
|  | hp-h       | 29           | 0.021 | 0.020  | 0.005 | 0.093 | 0.016          | 0.023          | 0.016    | 73.2             |
|  | scs        | 20           | 0.020 | 0.022  | 0.000 | 0.030 | 0.016          | 0.025          | 0.007    | 34.5             |
|  | w12-18     | 17           | 0.035 | 0.031  | 0.019 | 0.084 | 0.027          | 0.039          | 0.015    | 43.3             |
|  | w2-25      | 16           | 0.021 | 0.021  | 0.010 | 0.037 | 0.017          | 0.024          | 0.006    | 28.7             |
|  |            |              |       |        |       |       |                |                |          |                  |
| <b>C<sub>3</sub>H<sub>8</sub></b><br>ppm | main grid  | 358          | 0.072 | 0.038  | 0.000 | 0.665 | 0.024          | 0.072          | 0.098    | 136.0            |
|  | background | 37           | 0.170 | 0.058  | 0.018 | 1.759 | 0.035          | 0.112          | 0.358    | 211.1            |
|  | hp-h       | 29           | 0.124 | 0.101  | 0.023 | 0.331 | 0.051          | 0.161          | 0.091    | 73.1             |
|  |            |              |       |        |       |       |                |                |          |                  |
| <b>CO<sub>2</sub></b><br>%               | main grid  | 358          | 0.36  | 0.25   | 0.00  | 2.21  | 0.18           | 0.40           | 0.33     | 90.6             |
|  | background | 37           | 0.31  | 0.21   | 0.13  | 1.33  | 0.17           | 0.34           | 0.25     | 80.7             |
|  | hp-g       | 36           | 0.28  | 0.20   | 0.11  | 1.43  | 0.16           | 0.33           | 0.24     | 85.7             |
|  | hp-h       | 29           | 0.37  | 0.23   | 0.13  | 2.74  | 0.19           | 0.35           | 0.47     | 129.9            |
|  | scs        | 20           | 0.16  | 0.16   | 0.02  | 0.21  | 0.14           | 0.18           | 0.04     | 27.9             |
|  | w12-18     | 17           | 0.23  | 0.21   | 0.13  | 0.57  | 0.16           | 0.24           | 0.10     | 44.3             |
|  | w2-25      | 16           | 0.45  | 0.40   | 0.16  | 0.87  | 0.31           | 0.52           | 0.22     | 49.1             |
|  |            |              |       |        |       |       |                |                |          |                  |
| <b>COS</b><br>ppm                        | main grid  | 219          | 0.171 | 0.000  | 0.000 | 1.697 | 0.000          | 0.338          | 0.256    | 149.9            |
|  | background | 36           | 0.209 | 0.000  | 0.000 | 0.852 | 0.000          | 0.415          | 0.249    | 119.1            |
|  | hp-h       | 29           | 0.104 | 0.000  | 0.000 | 0.436 | 0.000          | 0.254          | 0.152    | 146.0            |
|  |            |              |       |        |       |       |                |                |          |                  |
| <b>O<sub>2</sub></b><br>%                | main grid  | 358          | 21.7  | 21.7   | 19.4  | 23.6  | 21.2           | 22.3           | 0.8      | 3.6              |
|  | background | 37           | 21.7  | 21.6   | 19.4  | 23.3  | 21.1           | 22.5           | 0.9      | 4.1              |
|  | hp-g       | 36           | 21.3  | 21.2   | 18.5  | 23.9  | 20.8           | 21.8           | 0.9      | 4.5              |
|  | hp-h       | 29           | 21.7  | 21.8   | 20.0  | 23.0  | 21.1           | 22.3           | 0.8      | 3.6              |
|  | scs        | 20           | 21.7  | 21.7   | 20.3  | 22.8  | 21.4           | 22.0           | 0.6      | 2.7              |
|  | w12-18     | 17           | 21.4  | 21.3   | 20.6  | 22.6  | 21.0           | 21.7           | 0.6      | 2.6              |
|  | w2-25      | 16           | 21.5  | 21.5   | 19.7  | 23.2  | 21.0           | 22.0           | 0.9      | 4.1              |
|  |            |              |       |        |       |       |                |                |          |                  |
| <b>N<sub>2</sub></b><br>%                | main grid  | 358          | 77.7  | 77.6   | 70.3  | 85.0  | 76.4           | 79.1           | 2.1      | 2.7              |
|  | background | 37           | 78.1  | 78.1   | 73.1  | 82.8  | 77.2           | 79.1           | 1.9      | 2.5              |
|  | hp-g       | 36           | 77.2  | 77.1   | 71.4  | 81.7  | 75.7           | 78.5           | 2.3      | 2.9              |
|  | hp-h       | 29           | 76.7  | 76.5   | 71.0  | 80.5  | 75.6           | 78.0           | 2.3      | 3.0              |
|  | scs        | 20           | 76.8  | 77.1   | 72.6  | 80.0  | 75.7           | 77.6           | 1.6      | 2.1              |
|  | w12-18     | 17           | 76.6  | 76.3   | 74.9  | 79.1  | 75.9           | 76.8           | 1.2      | 1.5              |
|  | w2-25      | 16           | 76.7  | 76.7   | 73.6  | 79.4  | 75.4           | 78.4           | 1.7      | 2.3              |
|  |            |              |       |        |       |       |                |                |          |                  |

*Table 4 Summary of main statistical parameters for selected field-measured gases and gamma spectrometry results at all studied sites in 2003, including, for comparative purposes, the main soil-gas grid. Note that hp refers to the horizontal profiles conducted over the river lineament, scs stands for salt collapse structure and w refers to the two decommissioned wells.*

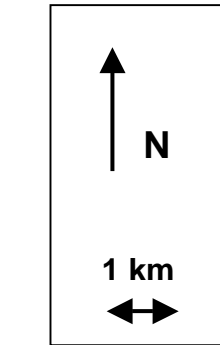
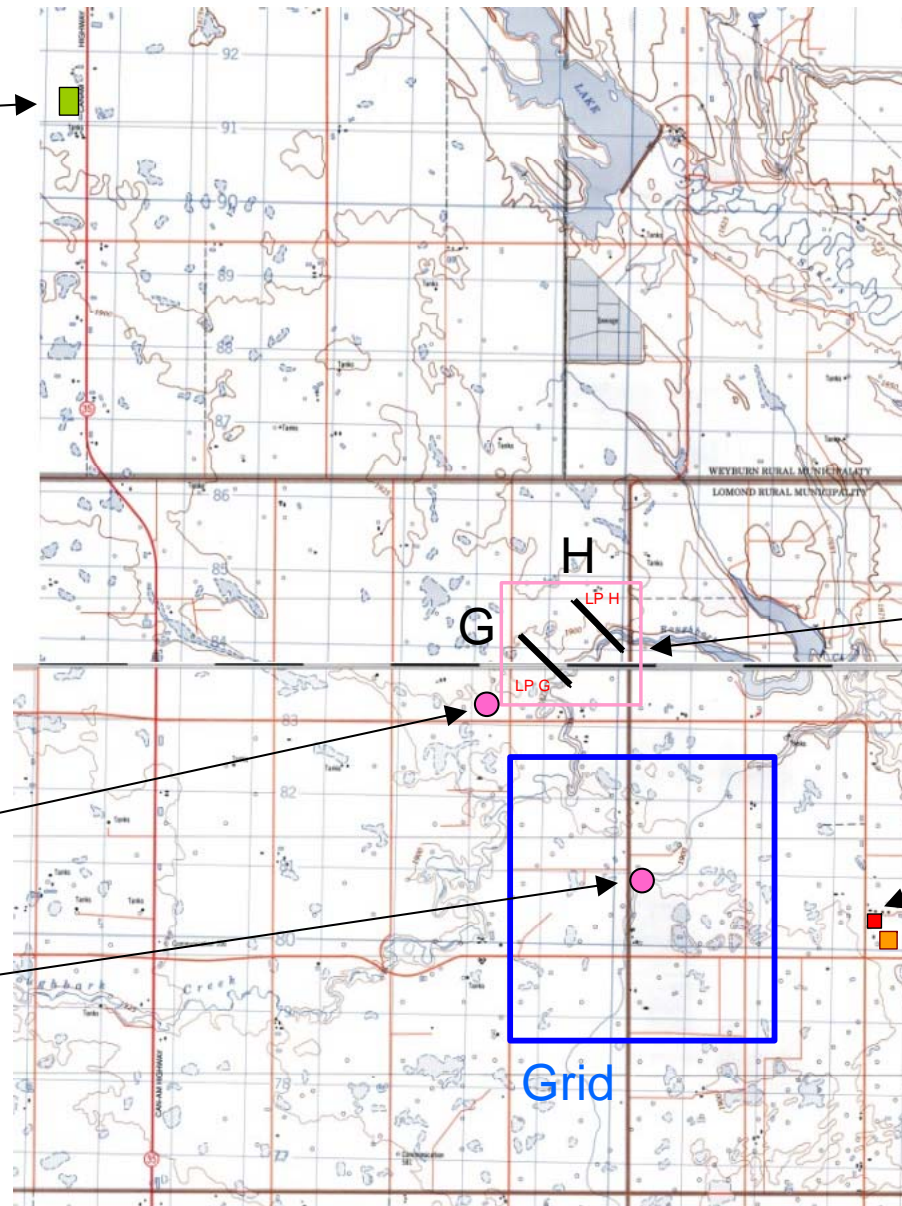
|                            | Site       | Valid Number | Mean | Median | Min. | Max. | Lower Quartile | Upper Quartile | Std.Dev. | Percent Std.Dev. |
|----------------------------|------------|--------------|------|--------|------|------|----------------|----------------|----------|------------------|
| <b>Rn</b>                  | main grid  | 360          | 15.2 | 13.8   | -6.9 | 82.0 | 7.7            | 20.5           | 11.8     | 77.4             |
| Bq l <sup>-1</sup>         | background | 37           | 19.9 | 19.6   | 9.5  | 32.4 | 15.7           | 24.3           | 5.6      | 28.2             |
|                            | hp-g       | 41           | 17.2 | 16.2   | 4.4  | 34.0 | 14.2           | 19.2           | 6.0      | 34.7             |
|                            | hp-h       | 43           | 15.7 | 14.7   | 6.1  | 28.6 | 10.9           | 20.5           | 6.1      | 39.2             |
|                            | scs        | 20           | 14.4 | 14.4   | 3.8  | 23.5 | 9.5            | 19.3           | 6.2      | 43.1             |
|                            | w-12-18    | 17           | 7.0  | 7.6    | 0.0  | 16.3 | 4.2            | 10.2           | 4.7      | 66.9             |
|                            | w2-25      | 17           | 20.1 | 18.7   | 9.9  | 34.1 | 15.1           | 24.6           | 7.9      | 39.2             |
| <b>Tn</b>                  | main grid  | 360          | 21.0 | 20.0   | 4.3  | 55.2 | 14.5           | 25.9           | 8.9      | 42.3             |
| Bq l <sup>-1</sup>         | background | 37           | 24.8 | 23.3   | 12.0 | 50.6 | 16.7           | 30.8           | 9.4      | 37.8             |
|                            | hp-g       | 41           | 19.5 | 18.3   | 7.4  | 40.2 | 12.1           | 25.5           | 8.6      | 44.1             |
|                            | hp-h       | 43           | 18.5 | 16.4   | 7.5  | 39.1 | 12.9           | 24.0           | 7.6      | 41.1             |
|                            | scs        | 20           | 19.4 | 18.9   | 9.1  | 32.5 | 13.7           | 26.1           | 6.6      | 33.9             |
|                            | w-12-18    | 17           | 18.1 | 17.6   | 7.2  | 29.2 | 14.5           | 22.2           | 6.2      | 34.2             |
|                            | w2-25      | 17           | 22.9 | 22.6   | 7.4  | 38.3 | 16.5           | 29.8           | 9.2      | 40.0             |
| <b>CO<sub>2</sub> flux</b> | main grid  | 359          | 3.0  | 2.4    | 0.1  | 16.2 | 1.5            | 3.9            | 2.4      | 78.6             |
| g/m <sup>2</sup> /d        | background | 37           | 2.3  | 1.7    | 0.4  | 7.8  | 1.1            | 2.8            | 1.8      | 76.7             |
| <b>Total gamma</b>         | main grid  | 7515         | 44.6 | 44.0   | 29.6 | 63.9 | 41.0           | 47.3           | 5.4      | 12.0             |
| cps                        | background | 1838         | 48.2 | 48.7   | 24.4 | 55.1 | 47.3           | 50.1           | 3.9      | 8.2              |
| <b>K</b>                   | main grid  | 7515         | 1.3  | 1.3    | 0.6  | 1.9  | 1.2            | 1.4            | 0.2      | 11.6             |
| %                          | background | 1838         | 1.4  | 1.4    | 1.0  | 1.8  | 1.3            | 1.5            | 0.1      | 10.0             |
| <b>U</b>                   | main grid  | 7515         | 2.2  | 2.0    | -0.2 | 7.6  | 1.5            | 2.8            | 1.1      | 50.7             |
| ppm                        | background | 1838         | 2.5  | 2.4    | 0.4  | 5.0  | 2.0            | 2.9            | 0.7      | 29.1             |
| <b>Th</b>                  | main grid  | 7515         | 5.4  | 5.3    | 1.7  | 10.4 | 4.6            | 6.3            | 1.2      | 22.9             |
| ppm                        | background | 1838         | 6.3  | 6.3    | 2.8  | 10.4 | 5.6            | 7.1            | 1.1      | 17.3             |

Minard's Farm  
Background site

Decommissioned wells

2:25 Failed casing  
Pumpjack in place

12:18  
Returned to farm land



Lineament profiles G & H

Encana site

Salt collapse structure

Figure 1. Locations of additional soil gas sites in relation to main grid

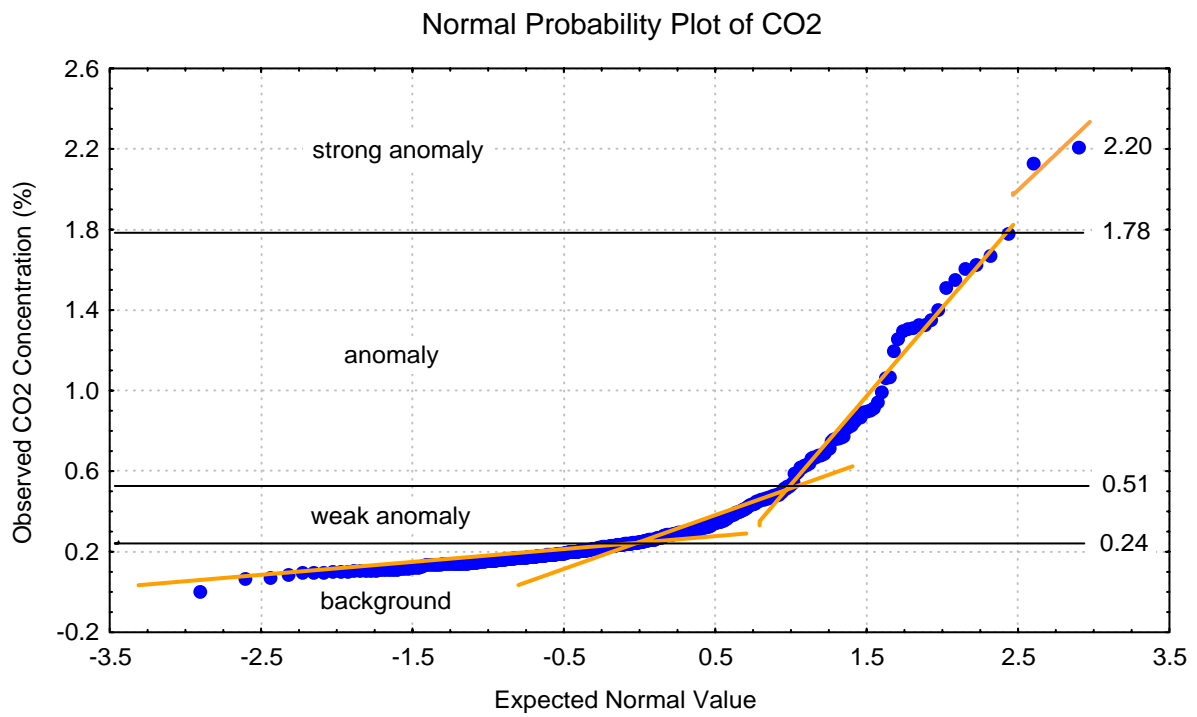


*Figure 2. Normal probability plot showing the method used for defining data set populations for laboratory analysed gases, with CO<sub>2</sub> values obtained over the main grid as an example. Note that the boundaries defined for the main grid have been used for the plotting of all studied sites in order to facilitate comparisons and to put the various values in a more regional context.*

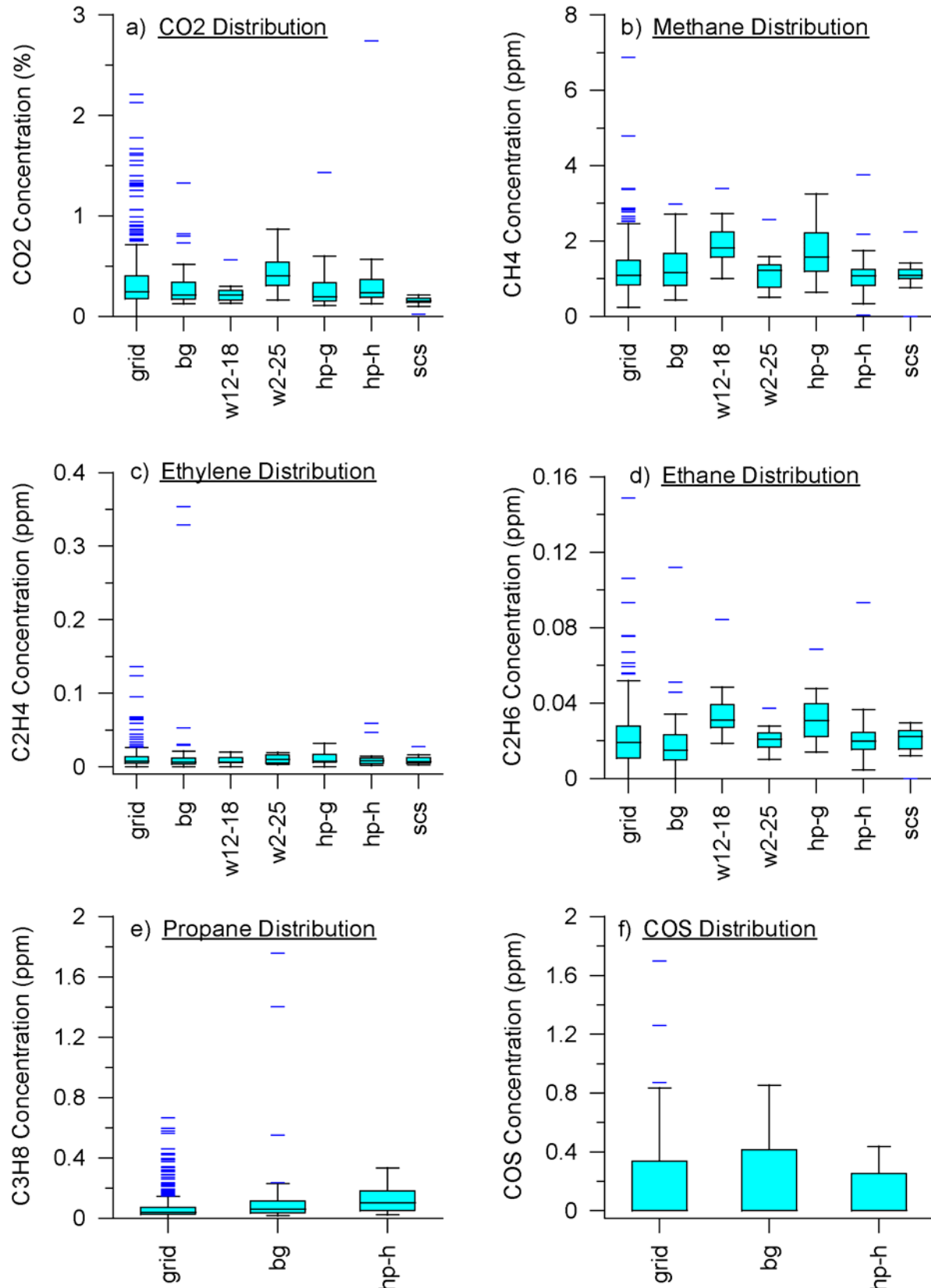


**Figure 3.** Box and whisker plot showing the statistical distribution of the laboratory datasets. The plot consists of a central horizontal line defining the median, a coloured box outlining the lower and upper quartiles, two 'whiskers' showing the 'normal' minimum and maximum values, and a series of blue lines defining outlier values. Abbreviations are as follows: grid - main grid over the CO<sub>2</sub> injection area, bg - background site, w - decommissioned wells, hp -horizontal profiles over the river lineament, scs - salt collapse structure.

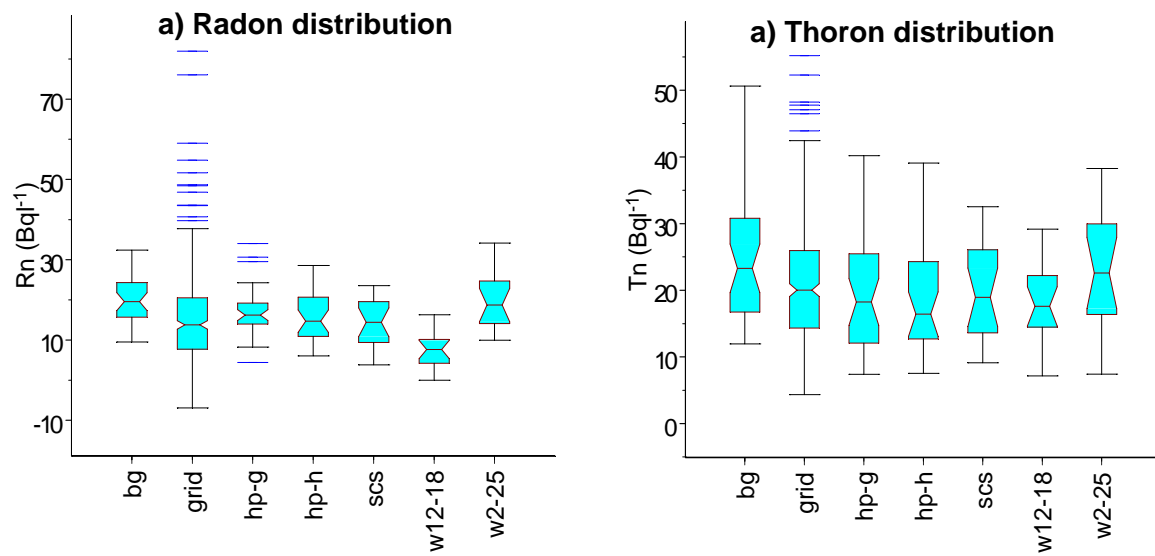


**Figure 4.** Box and whisker plot showing the statistical distribution of the BGS field data sets. The plot consists of a central horizontal line defining the median, a coloured box outlining the lower and upper quartiles, two 'whiskers' showing the 'normal' minimum and maximum values, and a series of blue lines defining outlier values. 'Notches' on the boxes show significant differences between the medians of groups at the approximately 95% confidence level. Abbreviations are as follows: grid - main grid over the CO<sub>2</sub> injection area, bg - background site, w - decommissioned wells, hp -horizontal profiles over the river lineament, scs - salt collapse structure.

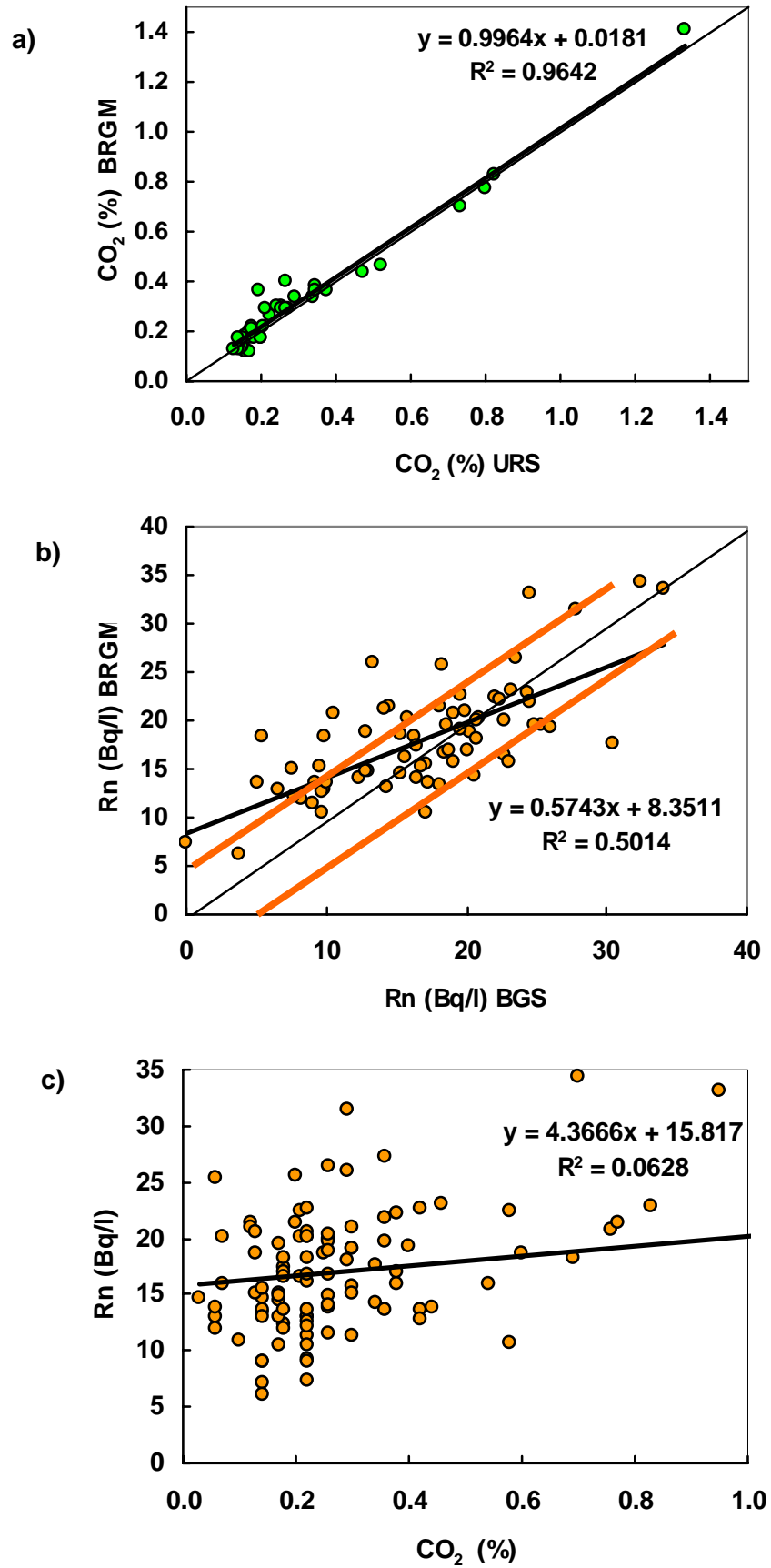
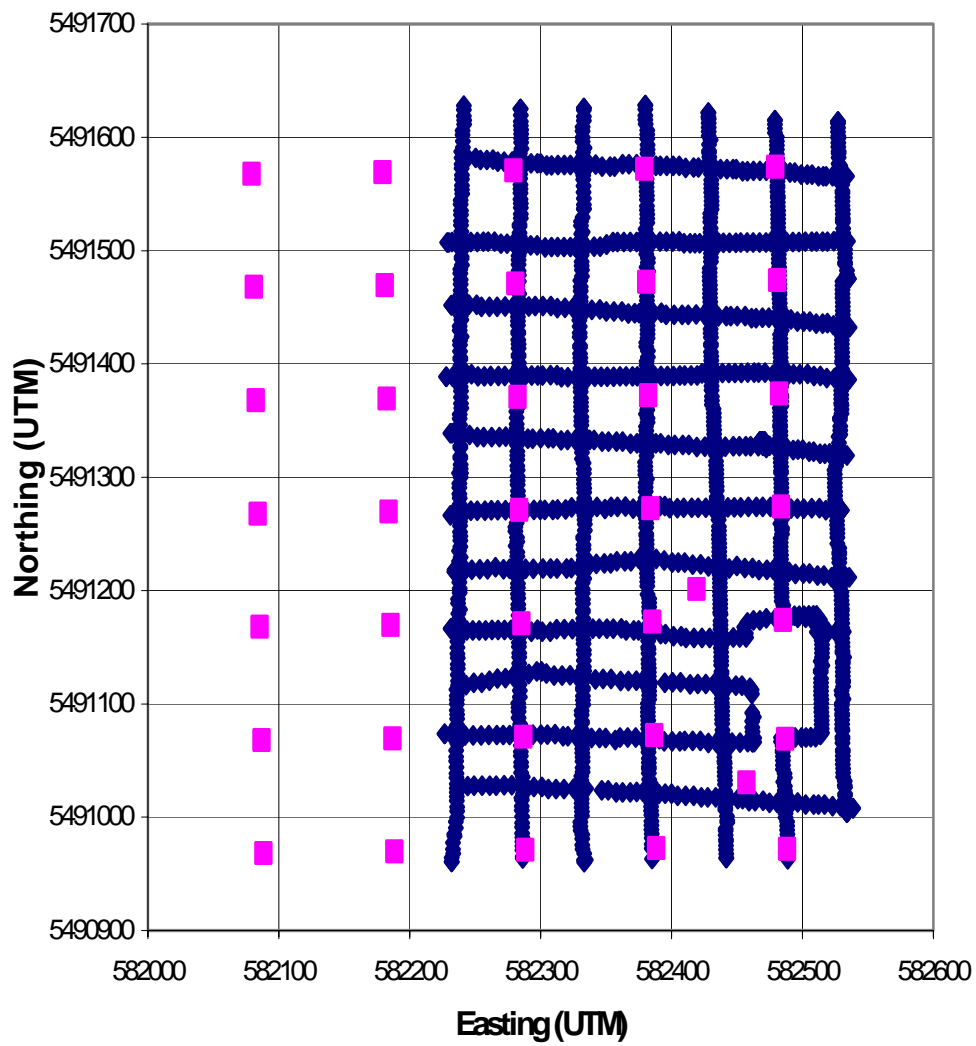
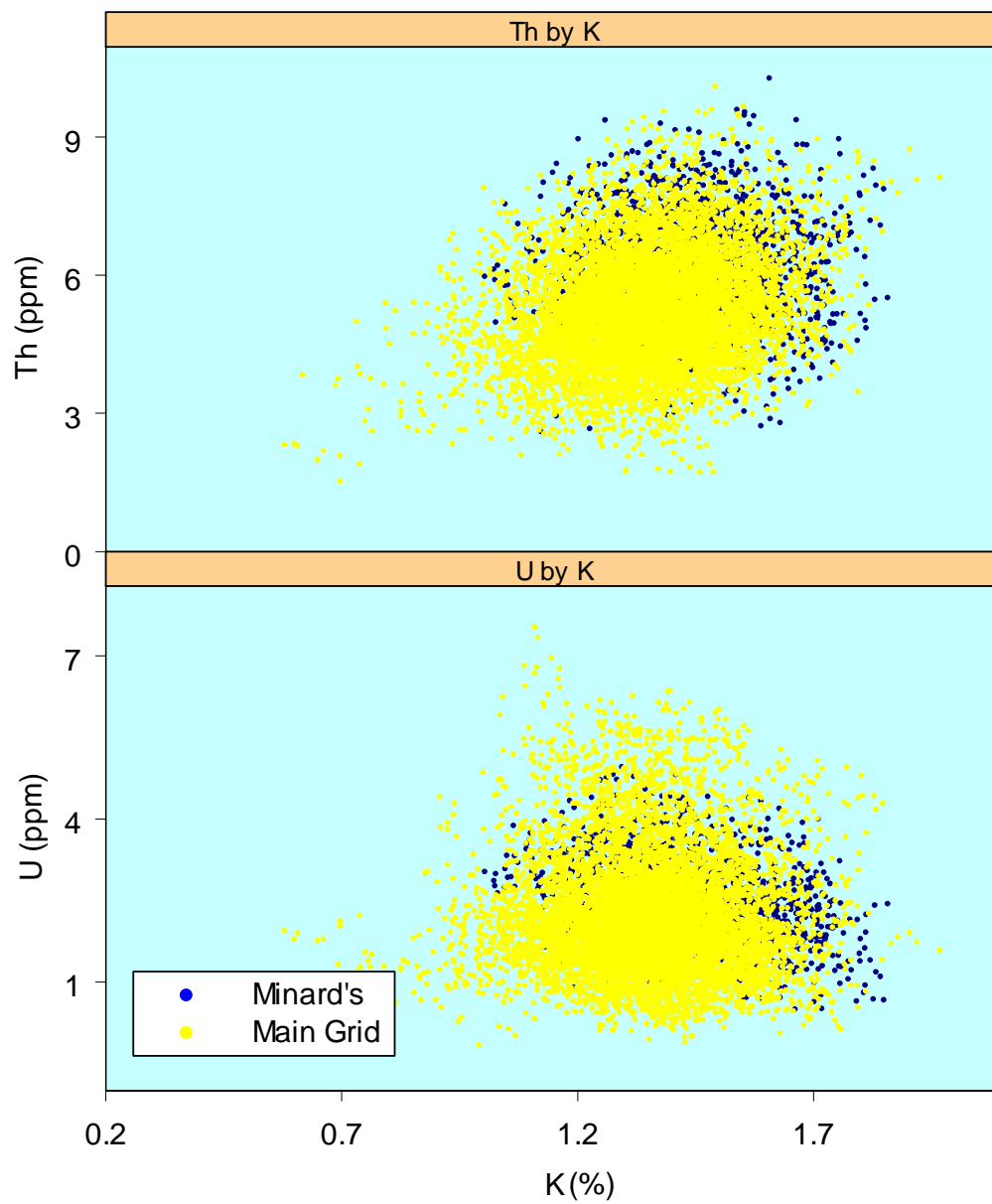


Figure 5. Data comparisons for additional soil gas work: a) Laboratory CO<sub>2</sub> (URS) v field CO<sub>2</sub> (BRGM); b) the two field Rn methods; c) Rn v CO<sub>2</sub>

## September 2003 Gamma spectrometry: Minard's Farm



*Figure 6. Gamma spectrometer traverses (black) and soil gas sample points (purple) for the background area near Minard's Farm*



*Figure 7. Comparison of gamma spectrometer data for the Background Site (Minard's Farm) and Main Grid areas*

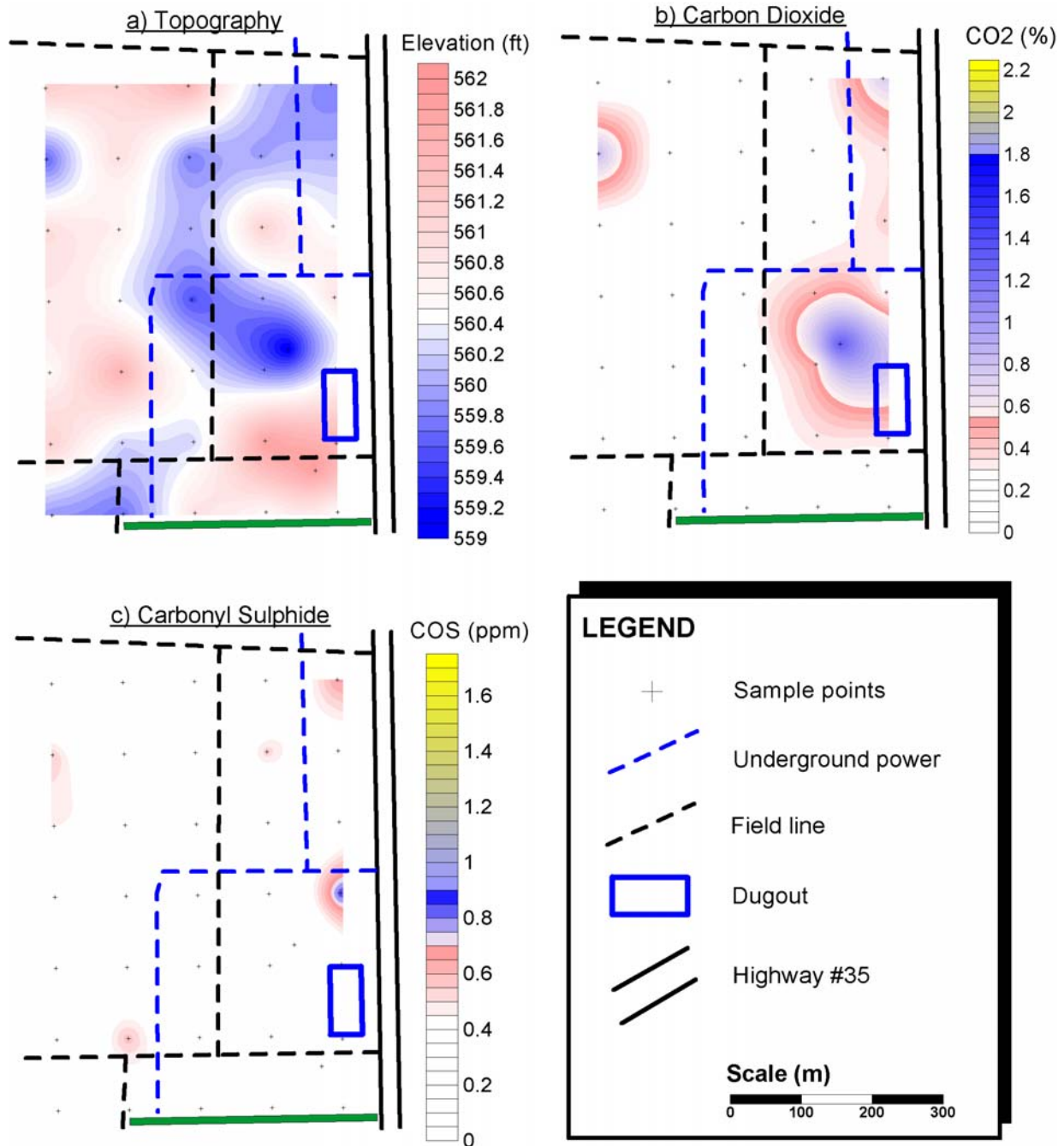


*Figure 8. Contour maps of data from the background site, which is located on the western side of Highway 35 approximately 10 km to the north east of the Encana site. Plots show elevation (a), CO<sub>2</sub> (b) and COS (c) distributions using the colour schemes and population divisions defined for the main grid data. Note that CO<sub>2</sub> values do not occur in the “highly anomalous” yellow field, and that all three spot anomalies occur in correspondence with elevation lows. COS values are consistently low compared to the main grid data. (continued on next page).*

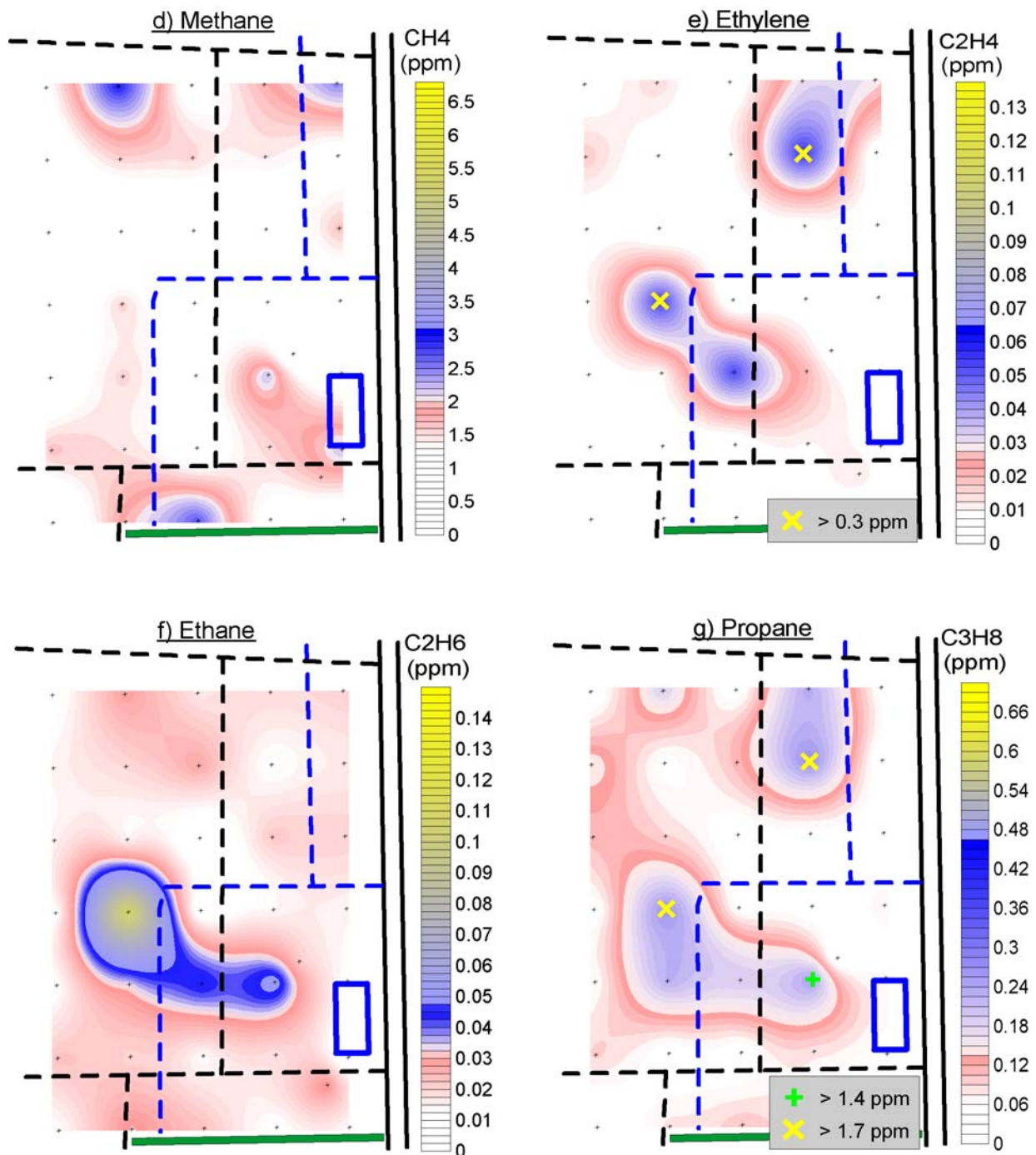


*Figure 8 (continued). Plots show methane (d), ethylene (e), ethane (f) and propane (g) distributions using the colour schemes and population divisions defined for the main grid data. Note that the three heavier hydrocarbons correspond very well amongst themselves, however that methane has a different distribution. Two values for ethylene and three for propane exceed the concentration ranges observed on the main grid, and thus these were removed from the data set for contouring purpose (in order to not give too much "weight" to a single point) and then these samples were plotted separately using symbols ("classed post").*

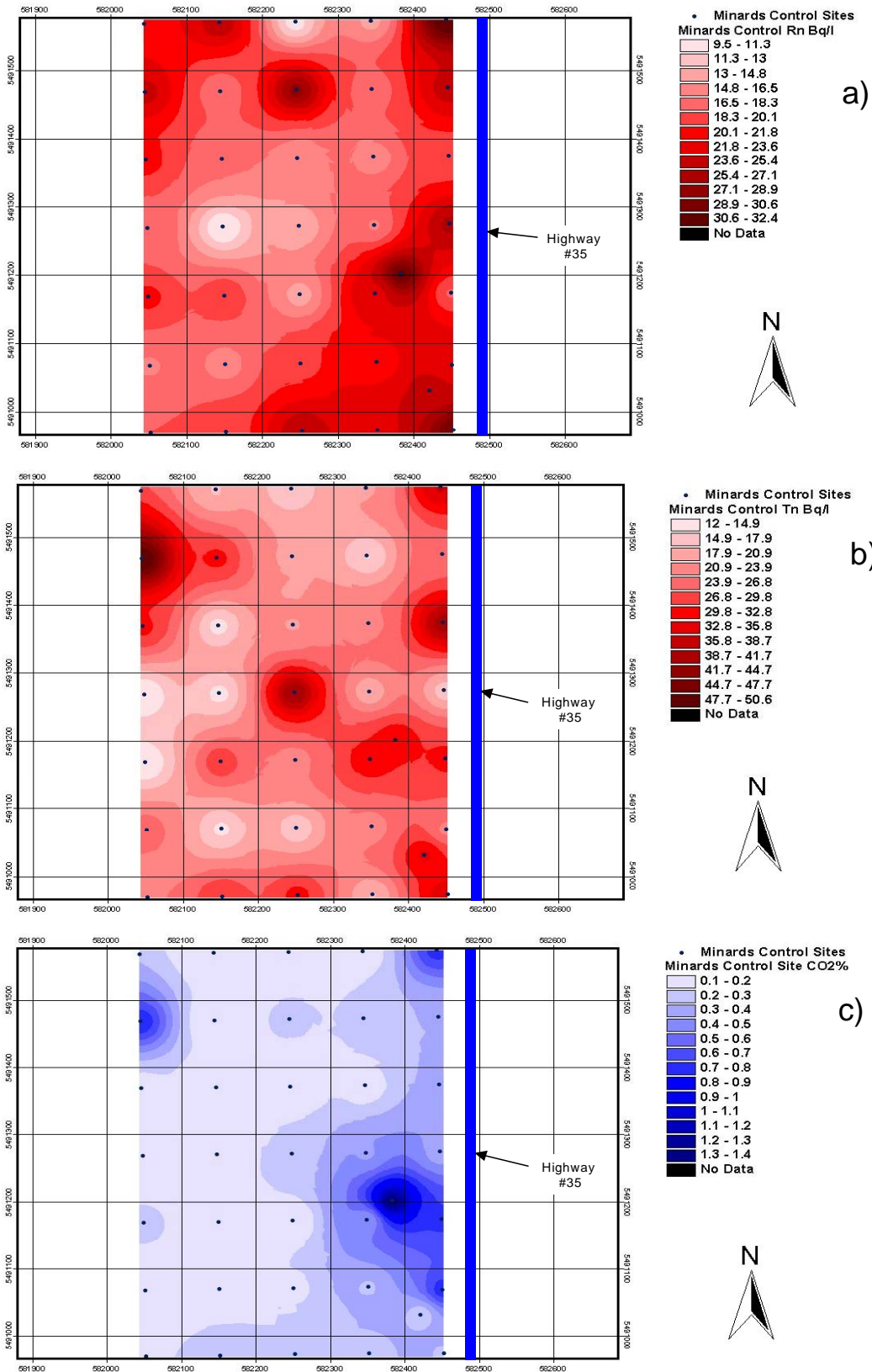


**Figure 9. Plots showing: a) Rn, b) Tn and c) field CO<sub>2</sub> for the background site at Minard's Farm. Note that there are broad similarities between the patterns of the gases, but also some differences in detail**

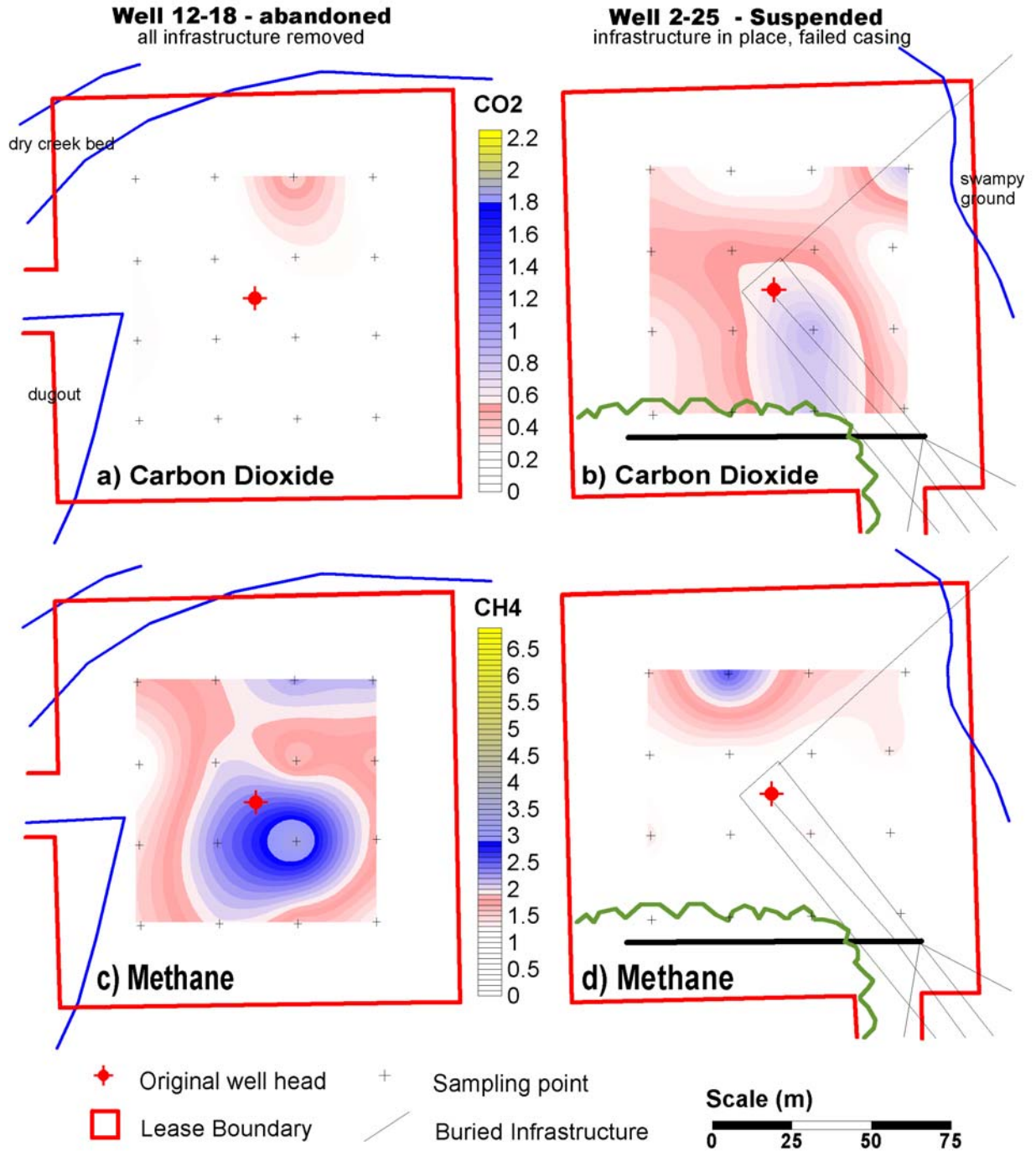


Figure 10. Contour maps of data from the two studied decommissioned wells. Plots show CO<sub>2</sub> and CH<sub>4</sub> distributions for well 12-18 (a and c) and for well 2-25 (b and d) using the colour schemes and population divisions defined for the main grid data. Note that CO<sub>2</sub> in well 2-25 (b) and CH<sub>4</sub> in well 12-18 (c) exhibit very few background values. (continued on next page).

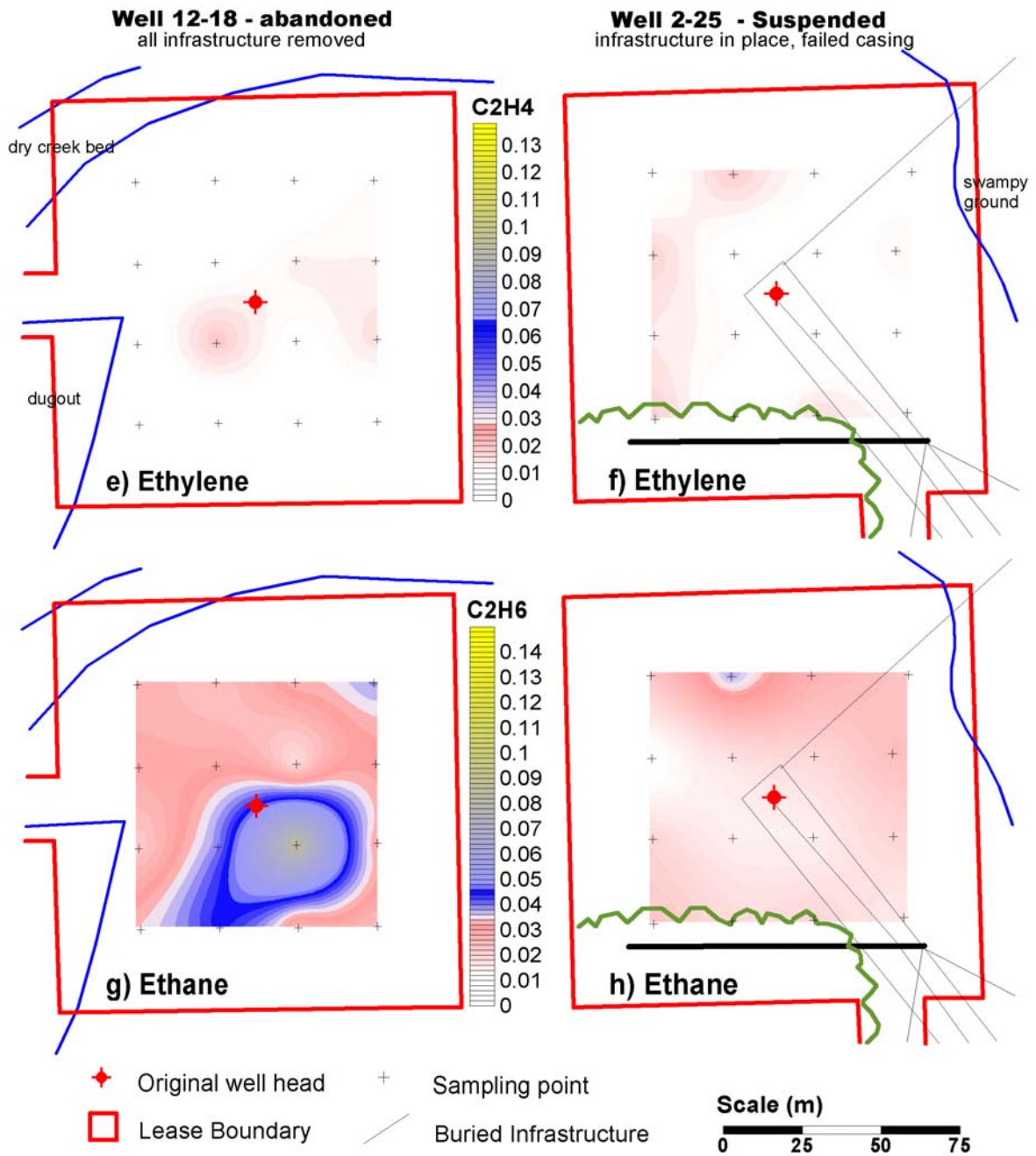
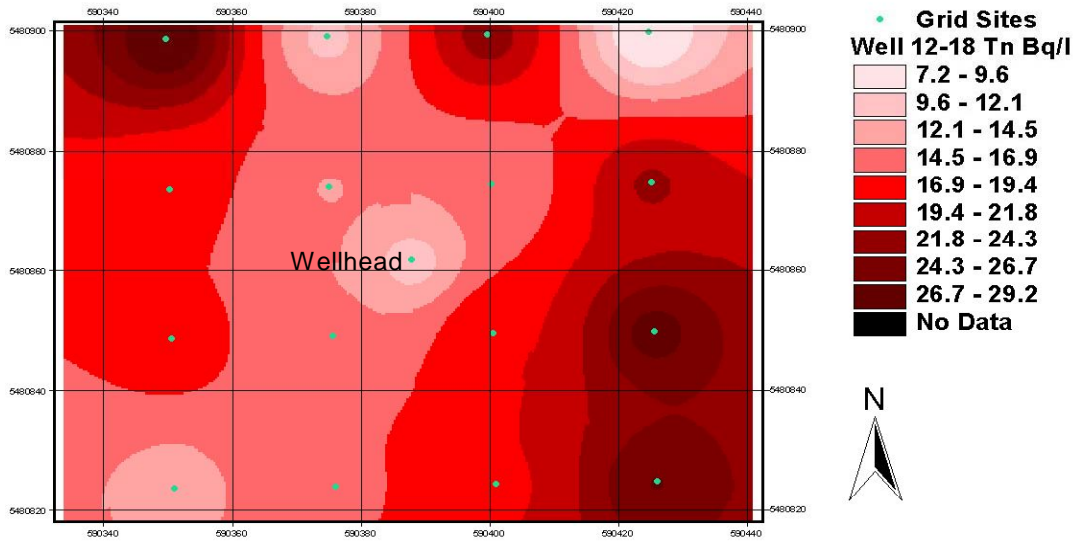


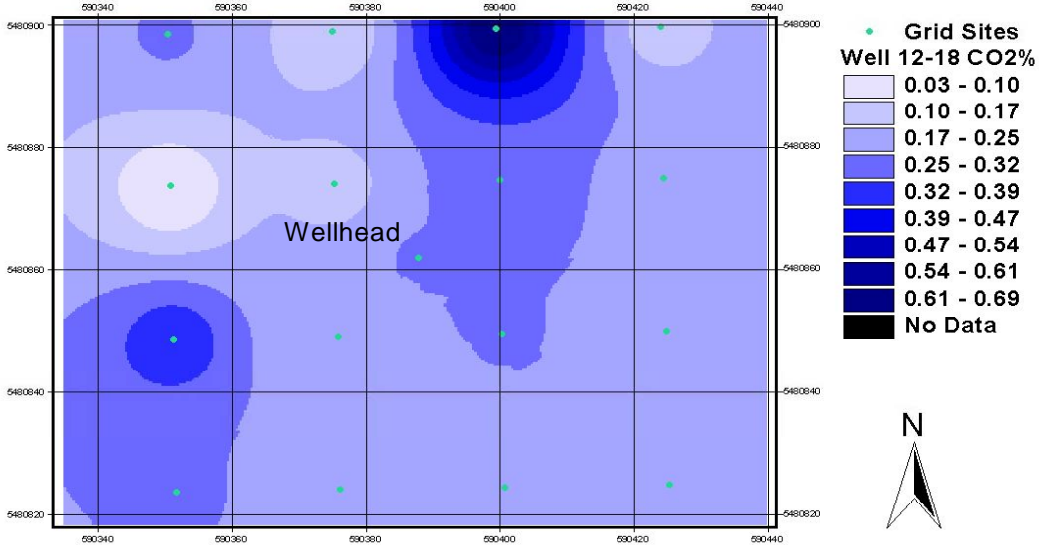
Figure 10 (continued) Plots show C<sub>2</sub>H<sub>4</sub> and C<sub>2</sub>H<sub>6</sub> distributions for well 12-18 (e and g) and for well 2-25 (f and h) using the colour schemes and population divisions defined for the main grid data. Note that the ethylene values are very low, however that ethane values exhibit very few background values and that the overall distribution is very similar to that of methane, particularly for well 12-18.

a)

Wellhead



b)



c)

*Figure 11. Contour maps of: a) Rn, b) Tn and c) field CO<sub>2</sub> distributions for abandoned well 12-18. Note the generally low levels of all gases and few features in common between CO<sub>2</sub> and the other gases*

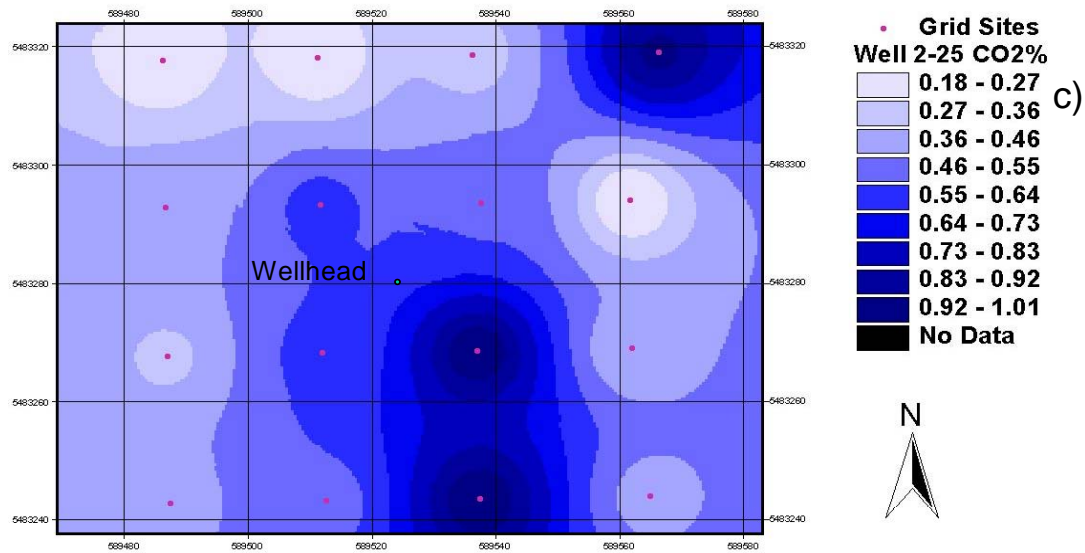
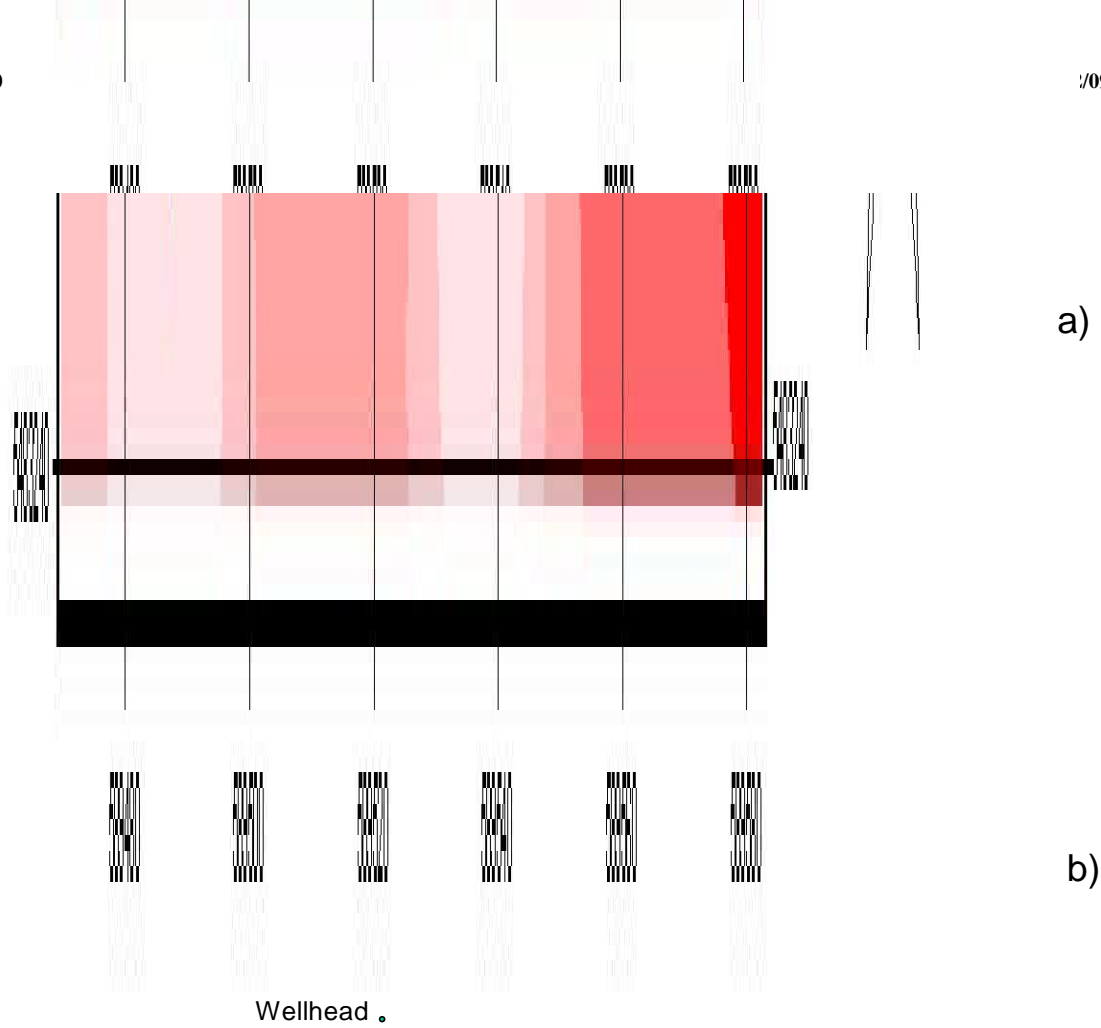
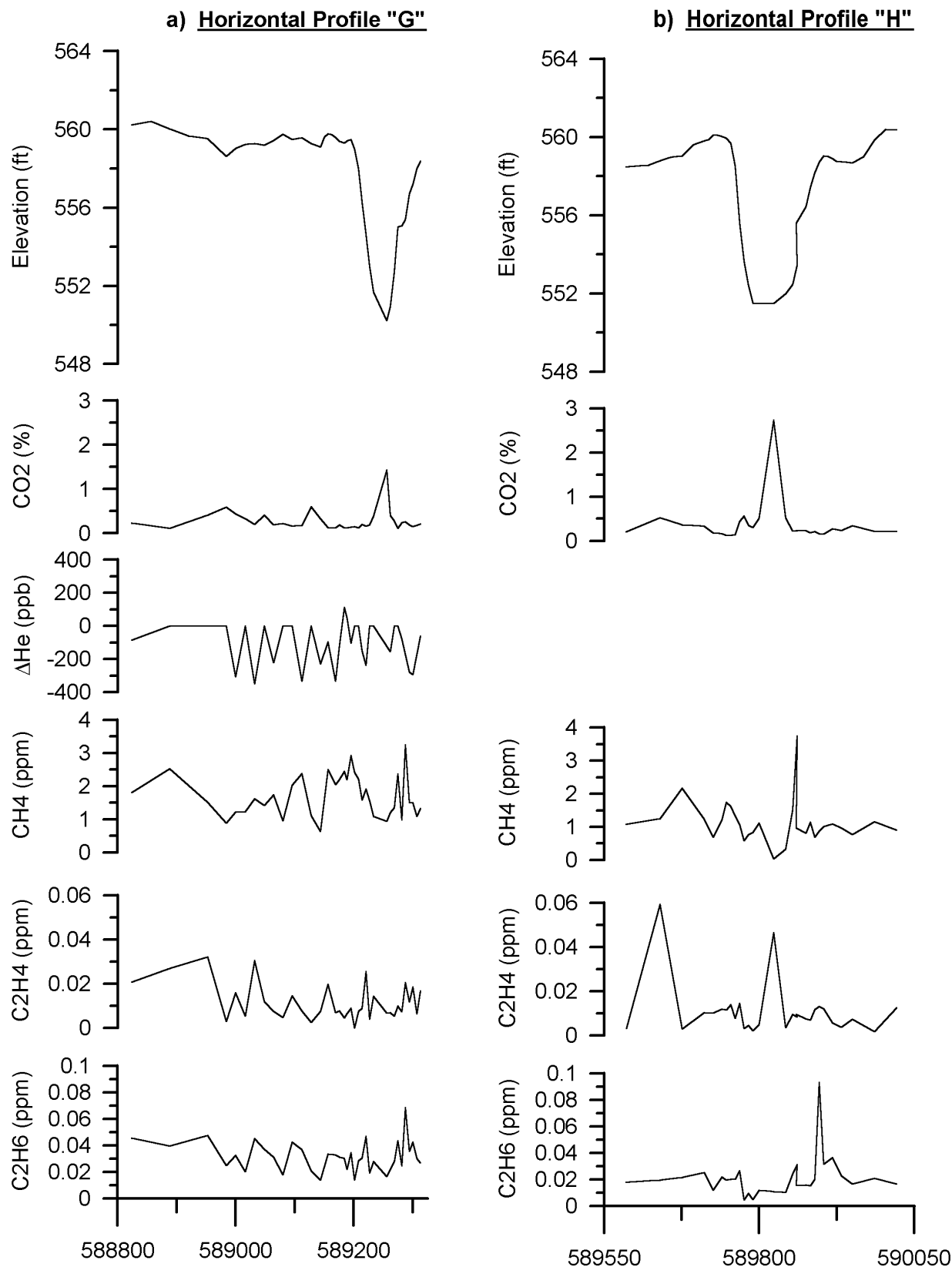
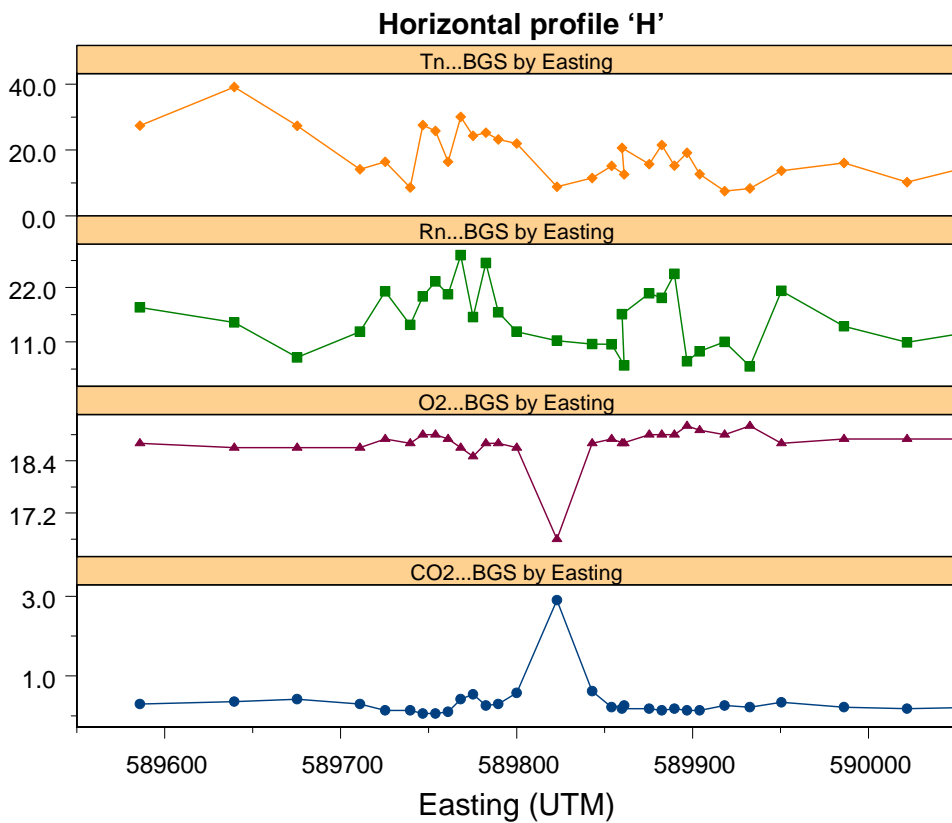
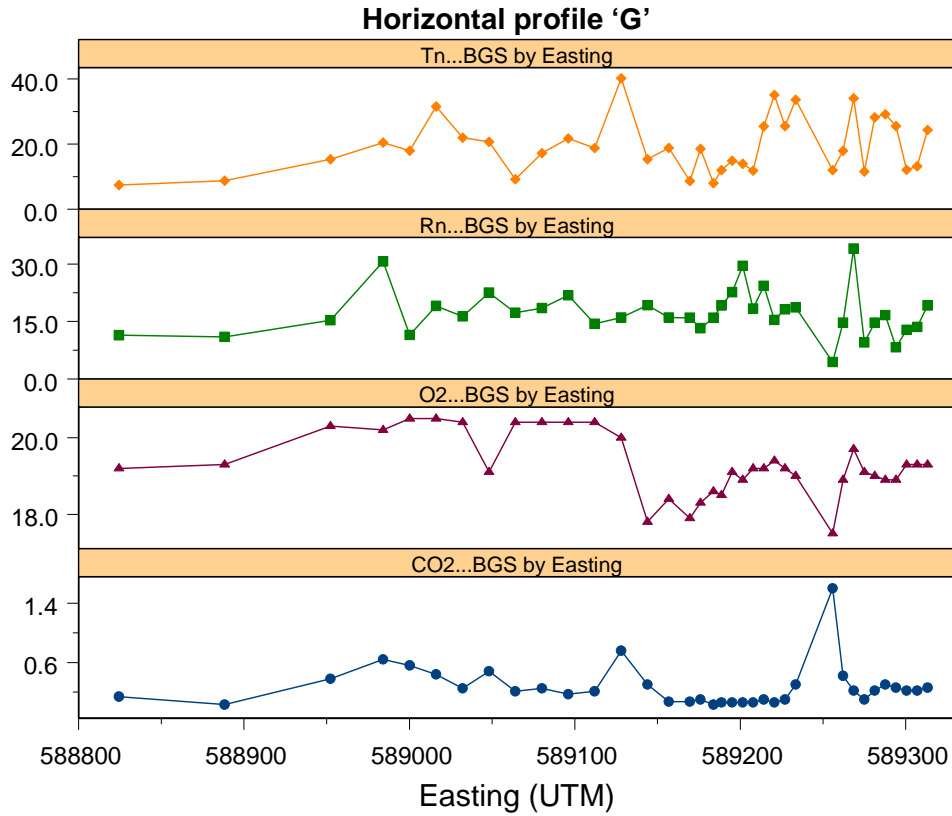


Figure 12. Contour maps of: a) Rn, b) Tn and c) field CO<sub>2</sub> distributions for abandoned well 2-25. Note that although two of the three points with highest CO<sub>2</sub> also have higher Rn and Tn, there are other relatively high Rn and Tn values associated with lower CO<sub>2</sub> levels



**Figure 13. Soil gas results from the two horizontal profiles performed across a river lineament (chosen by JD Mollard and Associates) to the north of the main soil gas grid. Note the correspondence between elevation and CO<sub>2</sub> concentrations for both profiles. The lack of correspondence with other gases (except one ethylene peak on profile H), however, implies a shallow biogenic origin for the CO<sub>2</sub> due to the moist, organic rich soil in the valley and in various small depressions.**



*Figure 14. Field soil gas results from the two horizontal profiles performed across a river lineament (chosen by JD Mollard and Associates) to the north of the main soil gas grid. Note the general lack of higher Rn and Tn where CO<sub>2</sub> is higher and the lower O<sub>2</sub> values, implying a biogenic origin for the CO<sub>2</sub> associated with vegetated areas of the valley floor and small depressions*

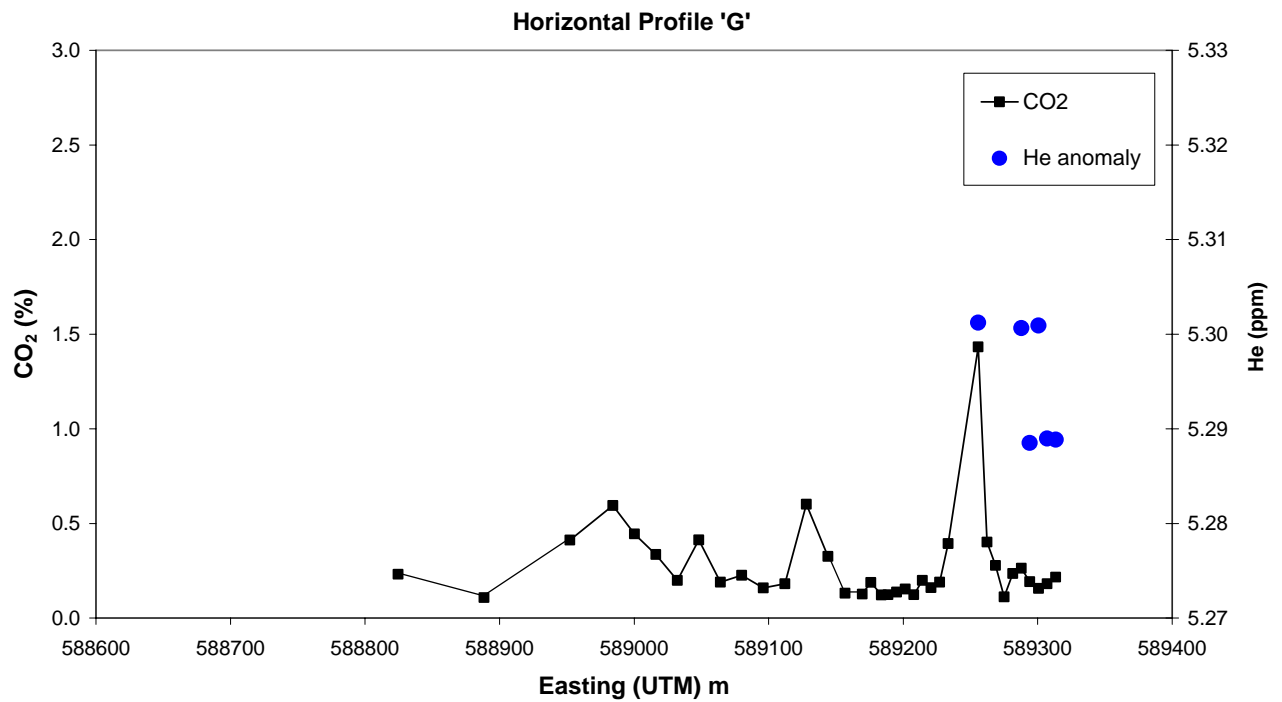


*Figure 15. Laboratory CO<sub>2</sub> and He (field laboratory) data for Profile G across the river lineament. Only He values clearly above the atmospheric level of 5.24 ppm are shown. Note the coincidence of a He anomaly with the main occurrence of higher CO<sub>2</sub>, but that other He anomalies are associated with very low levels of CO<sub>2</sub>*

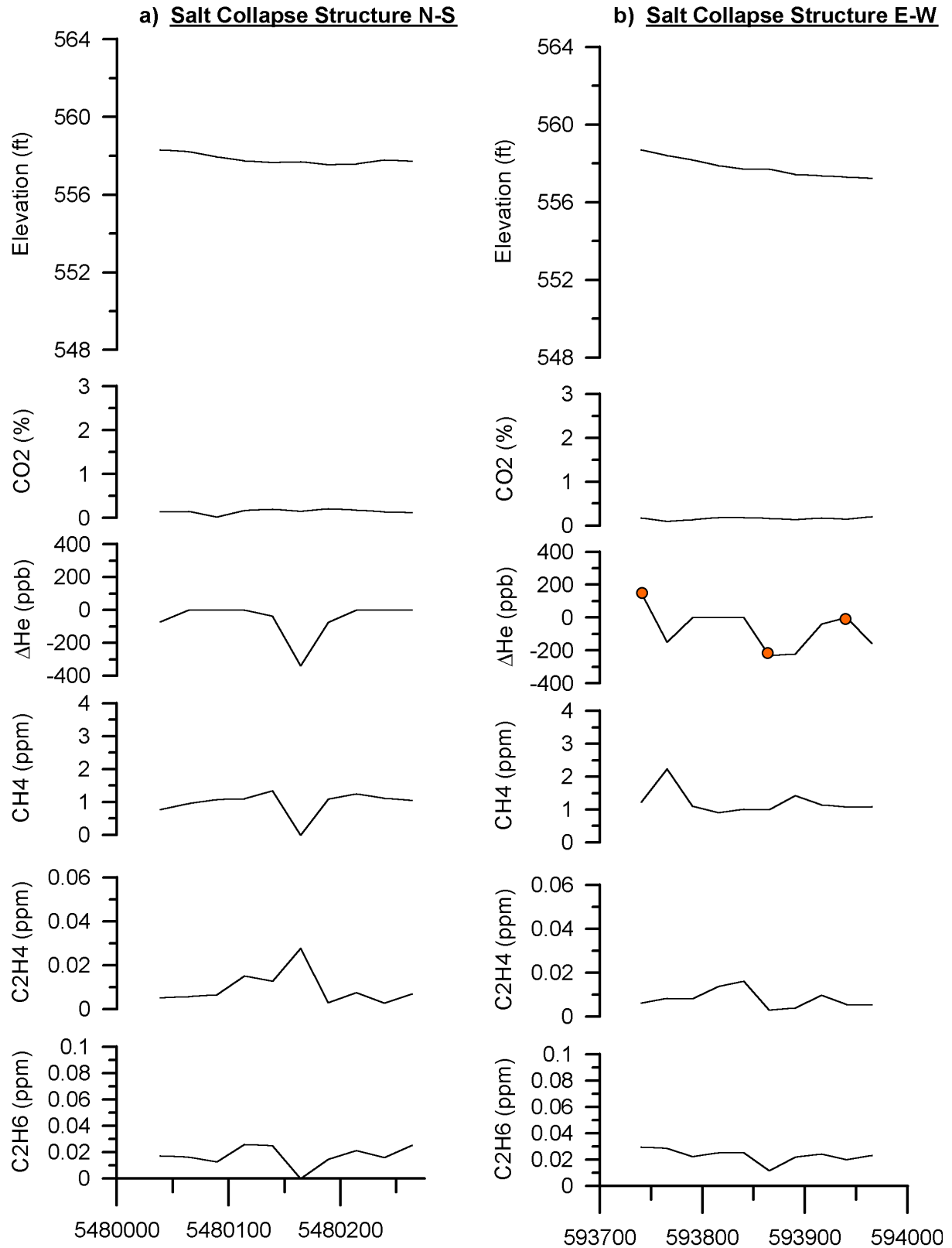


**Figure 16. Laboratory soil gas results from the two horizontal profiles performed across the salt collapse structure chosen by JD Mollard and Associates. Note that these data are plotted at the same scale as those in Figure 13 for comparative purposes. In general the lack of variation in the topography of this site is mimicked by the basically flat trends of the soil gas concentrations, particularly CO<sub>2</sub>. Three He anomalies from field laboratory data are shown (red dots) on the E-W He profile. They do not match any features in other gases**

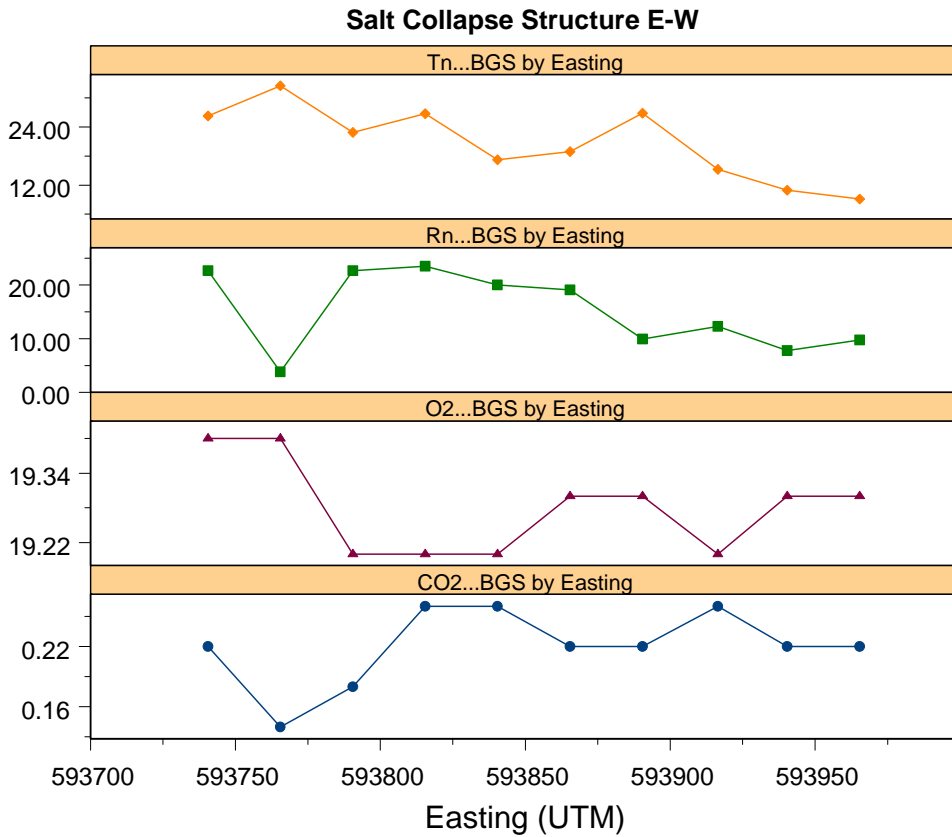
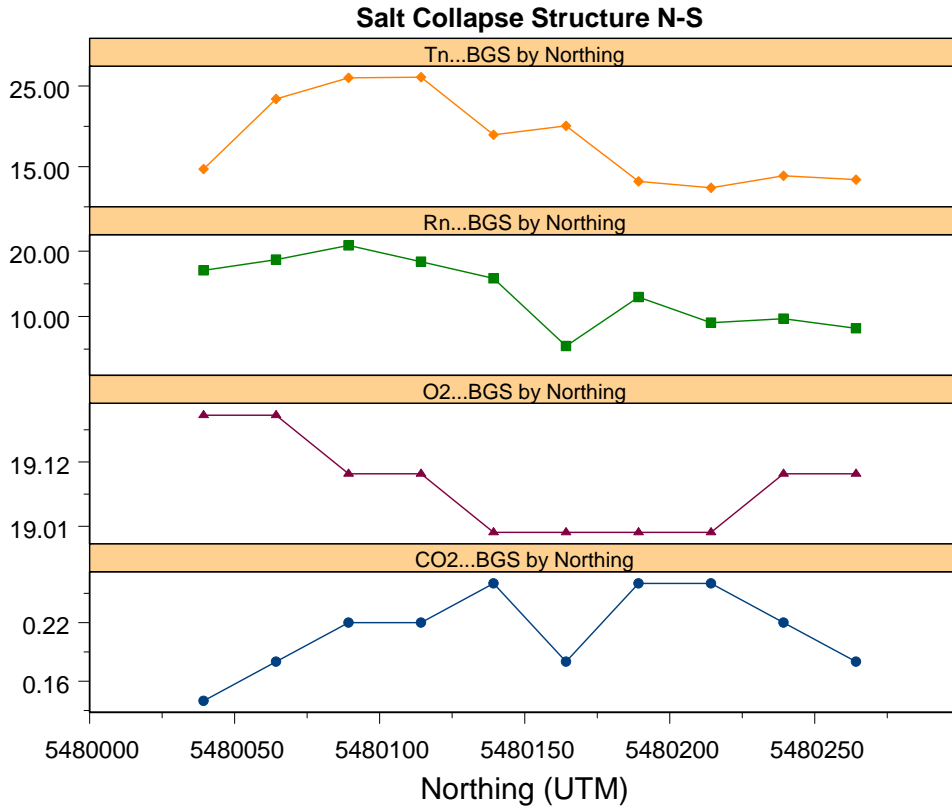


Figure 17. Field Soil gas results from the two horizontal profiles performed across the salt collapse structure chosen by JD Mollard and Associates.